

AD 693158



USE OF SOLID STATE ELECTROCHEMICAL TRANSDUCER  
TECHNIQUES FOR CONTROL OF THE POINT DEFECT  
STRUCTURE IN SOLIDS

by

M. S. Whittingham  
R. W. Helliwell  
R. A. Huggins

June, 1969

Department of Materials Science  
Stanford University  
Stanford, California

This document has been approved  
for public release and sale; its  
distribution is unlimited.

DDC  
RECEIVED  
SEP 15 1969  
C

SU-DMS-69-R-64

Department of MATERIALS SCIENCE  
STANFORD UNIVERSITY

USE OF SOLID STATE ELECTROCHEMICAL TRANSDUCER TECHNIQUES  
FOR CONTROL OF THE POINT DEFECT STRUCTURE IN SOLIDS

by

M.S. Whittingham, R.W. Helliwell, and R. A. Huggins

Final Technical Report

Office of Naval Research

Contract N00014-67-0112-0020

NR-032-506

June, 1969

Department of Materials Science

Stanford University

Stanford, California

Reproduction in whole or in part is permitted for any  
purpose of the United States Government. Distribution  
of this document is unlimited.

SU-DMS-69-R-64

## CONTENTS

<u>Chapters</u>		<u>Page No.</u>
	<u>PREFACE</u>	
I	<u>INTRODUCTION</u>	1
II	<u>X-RAY STUDIES OF THE STRUCTURE OF BETA ALUMINA AND RELATED PHASES</u>	6
III	<u>DEFECT EQUILIBRIA IN BETA ALUMINA AND RELATED PHASES</u>	27
IV	<u>IONIC CONDUCTIVITY IN BETA ALUMINA PHASES CONTAINING SILVER AND THALLIUM</u>	42
V	<u>IONIC TRANSPORT IN BETA ALUMINA PHASES CONTAINING SODIUM AND COPPER</u>	51

## PREFACE

This is a final report on work undertaken under Office of Naval Research Contract N00014-67-0112-0020.

This program was initiated on April 1, 1967 and terminated March 31, 1969 in conjunction with the initial principal investigator (Professor Robert A. Huggins) being granted a leave of absence to assume the post of Director for Materials Sciences with the Advanced Research Projects Agency. In his absence, responsibility for this program was assumed by Professor William D. Nix.

This report is divided into several reasonably independent chapters, representing the major areas in which a substantial amount of progress was made during the contract period.

Portions of the work undertaken which did not reach such a state of completion are not included. They were described in earlier Status Reports.

## CHAPTER I

### INTRODUCTION

It has recently become apparent that a number of the concepts and techniques that have been developed in connection with the use of high temperature solid state electrochemical cells might be very usefully applied to a variety of areas of materials science related to problems of structural characterization or control in solids. These involve the use of solid state phases, or groups of phases, having particular properties which can act as electrochemical transducers, whereby one type of physical quantity or measurement can be converted into that of another type. In this case, the transduction involves the conversion of various chemical quantities within a solid to externally measurable and controllable electrical quantities. Possible applications of the successful development of such techniques are both numerous and potentially of very great importance.

The intimate relationship between the point defect structure of solids and a wide range of physical properties is well known. Point defect-sensitive properties range all the way from various aspects of mechanical behavior, such as the yield stress, strain hardening, and ductility, through the more obvious electromagnetic properties such as electronic conduction, photoconductivity, luminescence, thermo-electric power, optical absorption, paramagnetic resonance, and the time-dependent low frequency magnetic properties such as the susceptibility, to the effect upon phase transformations, such as photodecomposition (the formation of photographic latent images) and the suppression of martensitic or shear type phase transformations in both metals and non-metals<sup>(1)</sup>. Because of their relevance to engineering applications, research on the physical properties of solids, and on the physical phenomena occurring within them, have been pursued with great vigor in recent years. In a number of cases the explicit relations between properties and the point defects present within a sample have been determined. More often than not, however, the understanding of these

relationships is still in a very preliminary stage, and much remains to be done. A very important aspect of this headlong rush to explore the physical properties of solids is that this work has progressed far ahead of activities related to either the characterization or the control of the defect structure responsible for these properties. In particular, relatively little attention has been given to the possibilities of structural changes after initial material preparation. This is particularly true in cases involving the use of single crystals, and tends to be more prevalent among those whose interests lie in the electromagnetic properties area and who work primarily with nonmetallics than with those whose interests are concerned more with metallic systems.

Many materials, both single crystalline and polycrystalline, are used in the "as grown" or "as fabricated" condition, with the resultant uncertainties in the point defect structure attendant to such procedures. A not insignificant fraction of such uncertainties relate to the history of samples as they pass through different chemical and temperature environments during their formation or processing. Such "environmental" influences can often be as important as "hereditary" factors in terms of the defect types, densities, and distributions actually present within solids.

Much is now known concerning the principles of point defect equilibria in solids from the definitive early German work of Wagner and Schottky<sup>(2-9)</sup> which has been more recently so well reviewed, systematized, and extended, primarily by the Dutch school<sup>(10-18)</sup>. This work has shown the numerous interactions between the concentrations of the various defects present in a solid, all of which are interrelated. However, by use of the concepts of thermodynamics, whose great advantage is its independence of the details of the microscopic state of a system, very powerful simplifications can be made. The Gibbs Phase Rule indicates, for example, that in a binary system the specification of one additional variable in addition to pressure and temperature results in the complete definition of the equilibrium state. As a result, the seemingly complex assembly of defect concentration relations can be completely specified, even without all of its details being known, by the control of one thermodynamic variable. In the case of a

ternary system, two such variables must be specified in order to completely define the equilibrium state.

As a result of this an increasing amount of research has been concerned with measurements of the properties of various materials as a function of the value of such a specified thermodynamic parameter. To date most of this work has involved equilibrating the solid with a controlled gas atmosphere containing the ingredients desired in known or measurable amounts. This method is not, however, always satisfactory for a number of reasons such as equilibration problems or because the desired partial pressure is outside the experimentally attainable range.

Instead of relying upon equilibration with a gas phase one can also establish the value of a thermodynamic variable by the use of electrochemical transducer techniques involving only solids. In a number of cases such techniques should be considerably more applicable than equilibration with a gas phase, and in addition, quantitative measurements involving the transport of material to or from the solid phase can be made by the use of electrochemical transducers which are not possible in the normal gas phase equilibration techniques.

Most of the applications of solid state electrochemical cells to date have been restricted by the sparsity of the presently available electrochemical transducers. To the present time techniques related to the control of only three ions have been extensively used. The transducers used are silver iodide (for silver), copper bromide (for copper), and either stabilized zirconia or thoria (for oxygen). These transducers are also very restrictive as to the temperature ranges in which they may be used.

It was the purpose of this work to search for suitable ionically conducting phases so as to extend the number of components which can be studied, practical reference electrodes, both for potential measurements and for ion reservoirs (sources and sinks), and viable experimental configurations.

This project involved primarily the investigation of the defect structure and ionic conduction properties of the beta alumina family.

These had been reported as being ionic conductors with unusually high diffusion rates for dissolved monovalent cations such as Na, Li, Ag, and Cu. Such indeed was found to be the case but there is little previous work on such highly ionically conducting materials and much effort had to be placed on finding suitable experimental techniques to measure the ionic conductivity. As the literature is plagued with results on poorly characterized materials it was felt highly desirable to make a full study of the crystal structure, defect model and ionic conductivity before moving on to study their applications as solid state electrochemical transducers.

An investigation was also made of the ionic conduction properties of various difluorides which preliminary indications showed likely to be highly ionic and might have relatively high diffusion rates. An NMR motional narrowing survey made in this laboratory of the fluorine nucleus in  $\text{CdF}_2$ ,  $\text{PbF}_2$ ,  $\text{CaF}_2$ ,  $\text{ZnF}_2$ ,  $\text{MnF}_2$ , and  $\text{LaF}_3$  also seemed to indicate movements of the fluoride ions in these systems. However, conductivity measurements on single crystals of  $\text{MgF}_2$ , using nickel electrodes which were believed to be reversible to fluoride ions, indicated a very low conductivity. Measurements on  $\text{ZnF}_2$  and  $\text{MnF}_2$  were complicated by apparent decomposition or interaction phenomena at the crystal surfaces. Investigations on these fluorides have been suspended because of personnel difficulties but it is still felt that these materials are possible candidates for solid state electrochemical transducers.

In the following chapters studies of the crystal structure, defect equilibria and ionic transport in the beta alumina system and related phases are discussed.

## REFERENCES

1. H.M. O'Brien, Jr., H.J. Levinstein and R.C. Sherwood, *J. Appl. Phys.* 37, 1438 (1966).
2. C. Wagner and W. Schottky, *Z. phys. Chem.* B11, 163 (1930).
3. C. Wagner, *Z. phys. Chem. Bodenst. Festband*, 177 (1932).
4. C. Wagner, *Z. phys. Chem.* B22, 181 (1933).
5. C. Wagner, *Z. Elektrochem.*, 39, 543 (1933).
6. W. Schottky, *Z. phys. Chem.* B29, 335 (1935).
7. W. Schottky, *Z. Elektrochem.*, 45, 33 (1939).
8. W. Schottky, Halbleiterprobleme 139 (1954).
9. W. Schottky, Halbleiterprobleme IV, 235 (1958).
10. F. A. Kröger and H. J. Vink, Solid State Physics, 3, 307 (1956).
11. H. Reiss, H.C. Fuller and F.J. Morin, *Bell System Tech. Jour.* 35, 535 (1956).
12. F. A. Kröger and H. J. Vink, Halbleiter und Phosphore, 17 (1958) (1956) Colloquium at Garmisch-Partenkirchen, ed. by M. Schon and H. Welker.
13. F. A. Kröger and H. J. Vink, *J. Phys. Chem. Solids* 5, 208 (1958).
14. F. A. Kröger and F. H. Stieltjes and H. J. Vink, *Philips Res. Repts.* 14, 557 (1959).
15. W. van Gool, *Philips Res. Repts. Suppl. No. 3* (1961).
16. H. J. Vink, Festkörperprobleme I, 1 (1962).
17. F. A. Kröger, Chemistry of Imperfect Crystals, North-Holland Publ. Co. (1964).
18. H. J. Vink, Festkörperprobleme IV, 205 (1965).

CHAPTER II

X-RAY STUDIES OF THE STRUCTURE OF BETA  
ALUMINA AND RELATED PHASES

M.S. WHITTINGHAM

R.A. HUGGINS

ABSTRACT

A group of  $\beta$  aluminas of the formula  $MA\ell_{11}O_{17}$ , where M is Li, Na, K,  $NH_4$ , Ag or Tl have been studied using x-ray techniques. The  $\beta$  alumina structure was confirmed for all the samples and the M ions were found to reside predominantly on the octahedral site as suggested by Beevers and Ross<sup>(2)</sup>, but in all cases the x-ray data indicated an excess of about 25% of M.

The structure of a sodium rich phase, which has a formula between  $Na_2O:Al_2O_3$  ratios of 1:5 and 1:6, was also determined but the positions of the sodium ions are still in doubt, as are the structural defects necessary to compensate for the additional positive charge in the sodium layers.

## INTRODUCTION

Much interest has recently been centered about fast ionic diffusion in compounds exhibiting the  $\beta$  alumina structure. In order to formulate a diffusion mechanism and to predict the most probable defects present it is essential to know the crystal structure with some accuracy. The results of investigations of the crystal structures of a number of  $\beta$  aluminas and related phases using x-ray techniques are the subject of this report.

Aluminum oxide,  $Al_2O_3$ , crystallizes in a number of forms, the most common being  $\alpha$  alumina (corundum) and  $\gamma$  alumina. The aluminum oxide formed from bauxite by the Bayer process has a structure known as  $\beta$  alumina. For a long time this was thought to be just another phase of alumina; not until 1936 when Beevers and Brohult<sup>(1)</sup> carried out accurate chemical analyses was this phase found to have the formula  $NaAl_{11}O_{17}$ . A year later Beevers and Ross<sup>(2)</sup> determined its crystal structure.

In the manufacture of aluminum oxide, a phase richer in sodium than  $\beta$  alumina was found. This phase is formed at about 1100°C and decomposes on heating at higher temperatures to give  $\beta$  alumina. It has variously been reported to have the composition  $NaAl_5O_8$ <sup>(3,4)</sup> and  $Na_2Al_{12}O_{19}$ <sup>(5)</sup>. Moreover, Scholder and Mansmann<sup>(5)</sup> reported the formation of analogous phases with gallium or iron instead of aluminum. Unfortunately, they also claimed that  $\beta$  alumina really has the formula  $M_2Al_{12}O_{19}$  and that all reaction products with the molar ratio  $M_2O:Al_2O_3$  are mixtures of  $M_2Al_{12}O_{19}$  and  $Al_2O_3$ . However, their paper shows a disregard for the conditions<sup>(6)</sup> necessary for the preparation of  $NaAl_{11}O_{17}$  as well as of the overwhelming structural evidence for its existence. As a sodium rich phase may indeed be present in many samples of what is supposed to be  $\beta$  alumina, a considerable part of this report will be concerned with the evidence for its existence and a study of its crystal structure.

Yamaguchi and Suzuki<sup>(7)</sup> have recently also reported the formation of a compound with the approximate composition  $Na_2O, 8Al_2O_3$ . This has

the same structure as  $\beta$  alumina and is probably just a stoichiometric variant rather than a separate phase. They also named the above and this phase  $\beta''$  and  $\beta'$  alumina respectively.

The only other reported sodium-containing phase in the aluminum-sodium-oxygen system is sodium aluminate,  $\text{NaAlO}_2$ <sup>(3)</sup>, which is found in orthorhombic and tetragonal forms<sup>(4)</sup>.

A modified version of the phase diagram determined for this system<sup>(6)</sup> is shown in Figure II-1; it is probable that this should be further revised to show some breadth to the phases  $\beta$  and  $\beta''$  as their structures are such that they would not be expected to have a narrow composition range.

#### THE ALPHA AND GAMMA STRUCTURES OF ALUMINA

Corundum,  $\alpha$  alumina, is the only phase of pure aluminum oxide stable at high temperatures and so may readily be formed by heating any other  $\text{Al}_2\text{O}_3$  structure above about 1000°C. It has the structure taken up by most trivalent metal oxides where the metal to oxygen radius ratio is less than 0.60. The oxygen ions are hexagonally close-packed with the aluminum ions in two-thirds of the octahedral sites.  $\gamma$  alumina is stable only at temperatures below 1000°C and its oxygen ions show cubic close-packing. The aluminum ions take up the positions of the Al and two-thirds of the Mg in the spinel  $\text{MgAl}_2\text{O}_4$ . Thus some of the aluminum ions are in octahedral and some in tetrahedral sites<sup>(8)</sup>.

#### THE STRUCTURES OF BETA ALUMINA AND MAGNETOPLUMBITE

Beevers and Ross<sup>(2)</sup> found that the crystal structure of  $\beta$  alumina consists of blocks of the  $\gamma$  alumina structure, hereafter called  $\gamma$  blocks, separated by loosely packed layers containing the sodium ions. In the  $\gamma$  blocks there are four layers of oxygen atoms, cubic close-packed, with aluminum ions occupying all the sites normally filled by both the Al and the Mg ions in the spinel  $\text{MgAl}_2\text{O}_4$ . This is in contrast to  $\gamma$  alumina where only two-thirds of the Mg sites are filled. The unit cell, which has the approximate parameters of  $a_0 = 5.59$  and  $c_0 = 22.5 \text{ \AA}$ , contains

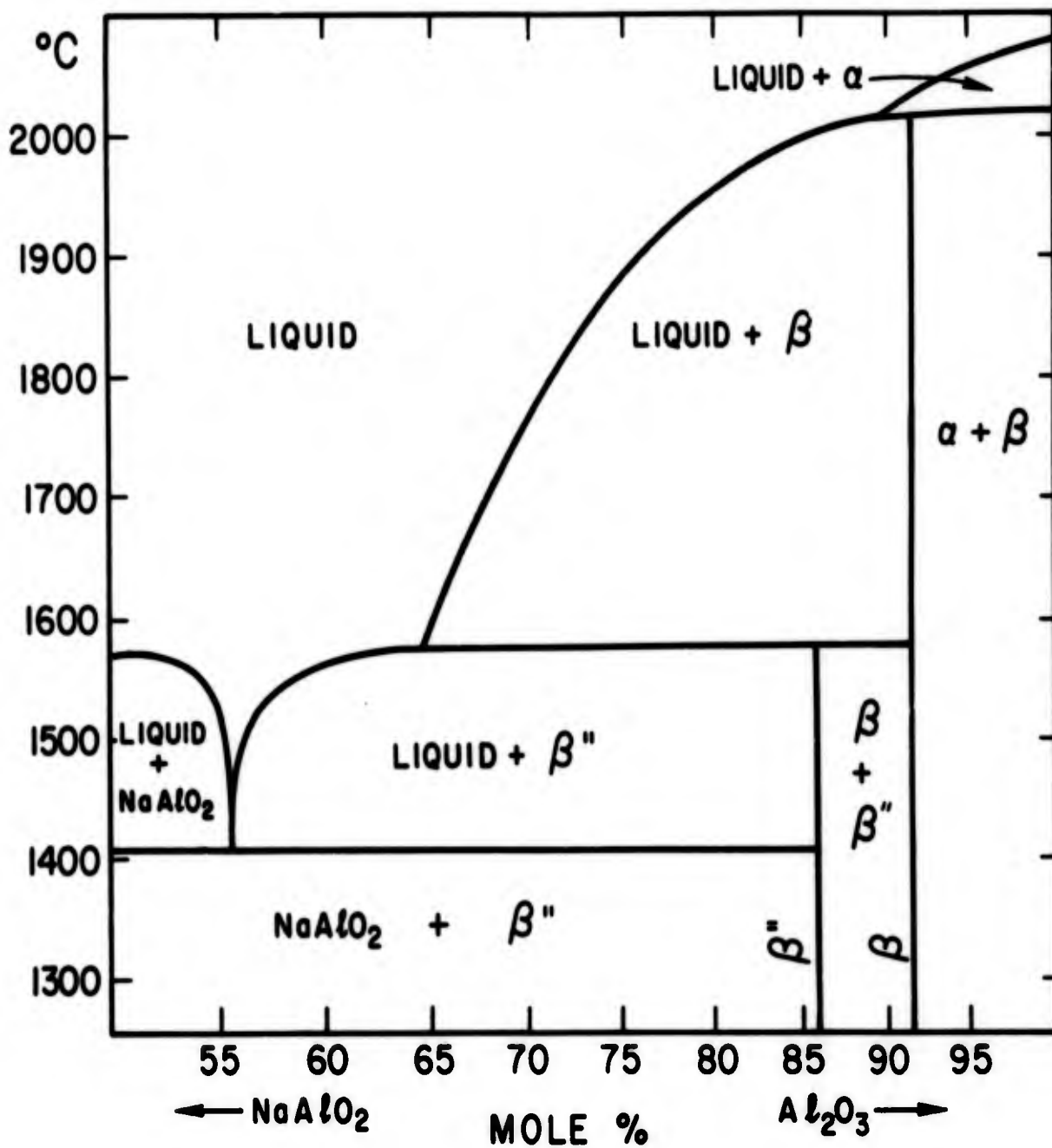


Figure II-1 Modified phase diagram of the NaAlO<sub>3</sub> - Al<sub>2</sub>O<sub>3</sub> system. (Note that the lines indicating the  $\beta$  and  $\beta''$  phase field should really be represented by areas).

two of these blocks separated by one connecting or bridging layer, which is a mirror plane of the structure.

In  $\beta$  alumina containing sodium the  $\gamma$  blocks take up 20 Al and 32 O ions so that only 1 Na, 1 O and 2 Al are in the bridging layer. The arrangement of these ions relative to those in the  $\gamma$  blocks is shown in Plate II-1. The aluminum ions in the bridging layers are in tetrahedral sites which are located adjacent to the vacant aluminum octahedral site in the  $\gamma$  block. There are two positions for the sodium atoms situated in the centers of triangles of oxygen atoms in the bridging layers. In the first of these the sodium ion has six nearest neighbor oxygen ions and in the second two. On the evidence of their x-ray data Beevers and Ross came to the conclusion that the first was the more probable. An overall view of the ions in the structure, which shows the emptiness of the bridging layers is given in Plate II-2.

Recently some single crystal determinations of the atomic positions in sodium  $\beta$  alumina have been reported. Felsche<sup>(9)</sup> and Bettman and Peters<sup>(10)</sup> found essentially the same positions as reported in the original investigation but with a slight puckering of the oxygen layers. Whereas the former considered deviations only in the c direction, Bettman and Peters considered deviations in all three directions relative to the ideal lattice. However Felsche used a sample which had been used in a glass tank for two years and reported no chemical analysis for either the major constituents or of any impurities, e.g., silicon, that might have been present. Thus the conclusions of his work, that there is about a two-third deficit of sodium and an appreciable oxygen deficit also in the bridging layer, must be considered as having questionable generality as both previous investigators and ourselves have found there to be a tendency for an excess rather than a deficit of sodium in sodium  $\beta$  alumina.

At about the same time as the structure of the above compound was being determined a number of investigations were being carried out on related divalent metal aluminates and ferrates<sup>(11-14)</sup>. Adelsköld<sup>(14)</sup>

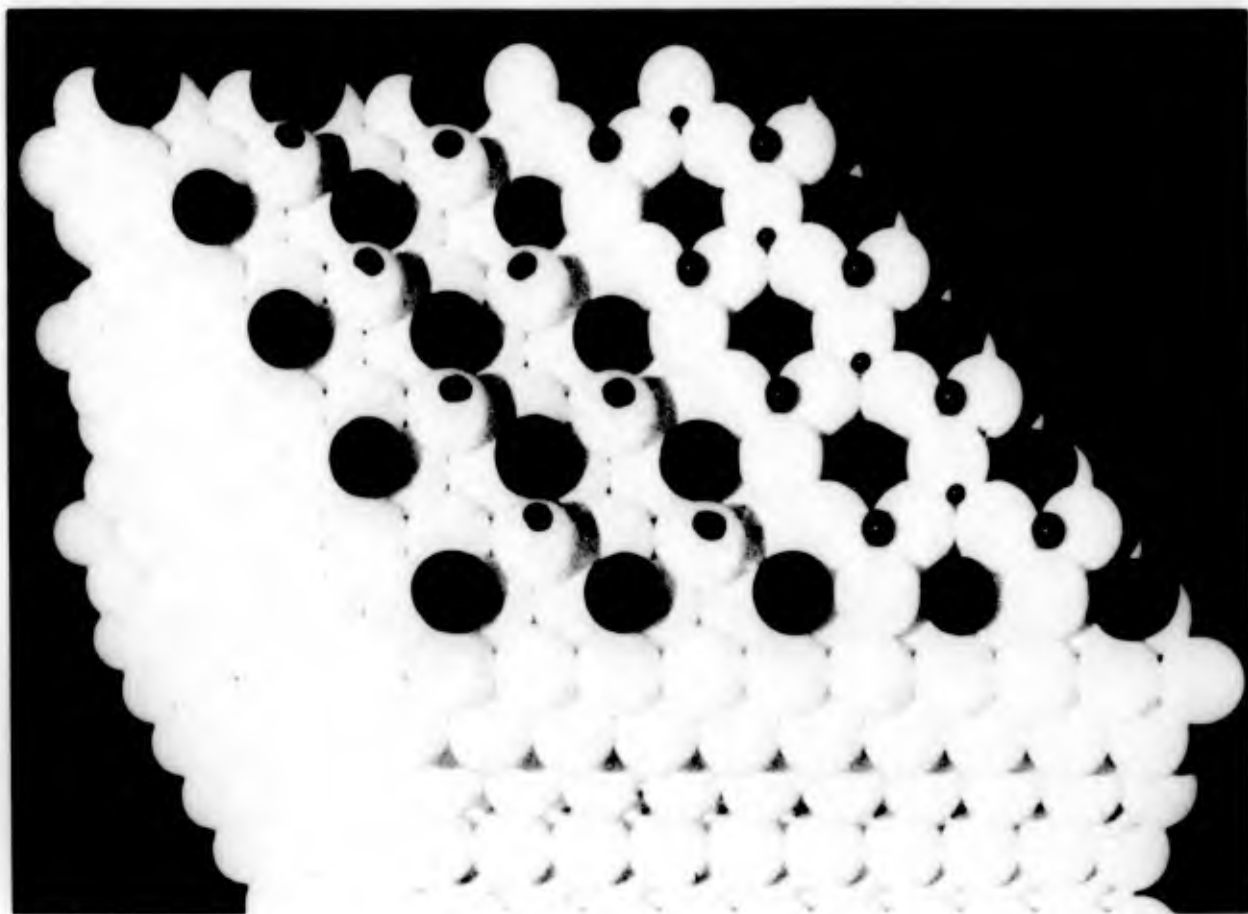


Plate II-1 Bridging Layer of the  $\beta$  Alumina and Magnetoplumbite Structures

Left Half:  $\beta$  alumina  $MA\lambda_{11}^{0}{}_{17}$

Right Half: Magnetoplumbite  $MFe_{12}^{0}{}_{19}$

Large black balls	$M^{+}$ or $M^{2+}$ ions
Black marks	$Al^{3+}$ ions in tetrahedral sites
Small black balls	$Fe^{3+}$ ions in octahedral sites
Tiny black balls	$Fe^{3+}$ ions in pentahedral sites
White balls	$O^{2-}$ ions

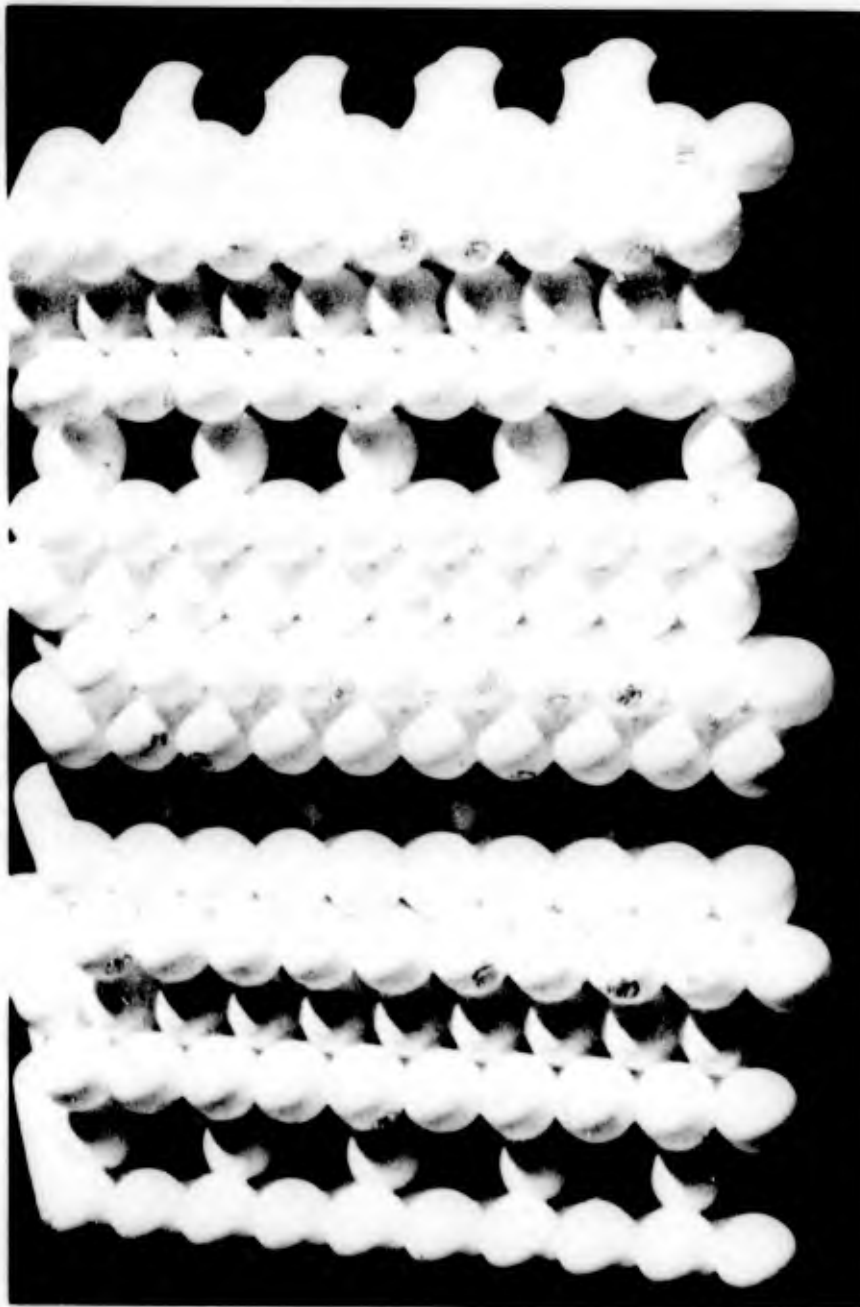


Plate II-2 Overall View of the  $\beta$  Alumina Structure

(The bridging layer next to the top contains no M ions to show the open structure of the lattice. Two ions in the model have been accidentally misplaced).

found the structures of these compounds, on the basis of a formula for magnetoplumbite of  $\text{PbFe}_{12}\text{O}_{19}$ , to be similar to  $\beta$  alumina, the only difference being in the bridging layers. The formula shows that there must be 1 Pb, 3 Fe, and 3 O in the bridging layer. The lead and oxygen ions form a close-packed lattice as shown in the right half of Plate II-1. Two of the iron atoms which are in the same positions, relative to the  $\gamma$  blocks, as the bridging aluminum ions in  $\beta$  alumina, are now in octahedral sites because of the different oxygen positions. The third iron atom is in the plane of the lead and oxygen ions and is in a site surrounded by five nearest neighbor oxygen ions. It can be clearly seen from Plate II-1 that there is no alternative site for the lead ions in this structure.

#### THE SODIUM RICH PHASE (SODIUM BETA PRIME ALUMINA)

When this study originated very little was known structurally about sodium  $\beta'$  alumina. Although reported in the Japanese literature<sup>(15)</sup> in 1943, the first work in the West was by Thery and Briancon<sup>(3)</sup>. They found that the x-ray pattern could be indexed assuming a hexagonal cell with a  $c_0$  parameter 1.5 times that of sodium  $\beta$  alumina and with the same  $a_0$  parameter. They suggested that the structure was similar to that of the ferrite  $\text{BaFe}_2^{\text{II}}\text{Fe}_{16}^{\text{III}}\text{O}_{27}$ <sup>(16)</sup>. This compound has a structure similar to magnetoplumbite but the  $\gamma$  blocks are six oxygen layers thick. However, their x-ray data do not support a structure with a c axis of  $n \times 16.4 \text{ \AA}$  but one with a c axis of  $n \times 11.4 \text{ \AA}$ , that is the same as sodium  $\beta$  alumina. Recently Yamaguchi and Suzuki<sup>(7)</sup> and Bettman and Peters<sup>(10)</sup> have investigated the structure of this compound. As their results are essentially the same as those found here further discussion of this structure will be delayed until later.

#### PROGRAM UNDERTAKEN

The purpose of this work was to confirm the  $\beta$  alumina structure for a number of  $\beta$  aluminas containing ions other than sodium and to attempt to explain some discrepancies which had been noticed in the intensities of

the diffraction lines relative to those expected for the Beevers and Ross structure. Furthermore, very little work has been performed to determine the actual positions of the alkali and other substitutional ions in the bridging layers and it was felt that by using a heavy atom, e.g., thallium, these positions could be identified unequivocally. In addition the structure of the phase richer in sodium than  $\beta$  alumina was investigated.

A sample of  $\text{CaAl}_{12}\text{O}_{19}$ , which has the magnetoplumbite structure, was studied as a test of the method used here and to verify that distortion within the  $\gamma$  blocks could be neglected. In this structure there is a unique site for the calcium ion so that the intensities of the diffraction can be calculated accurately.

#### MATERIALS PREPARATION

Single crystals and large crystalline bricks of sodium  $\beta$  alumina were obtained from The Carborundum Company, Falconer, New York. Only specimens that were visually free of a second phase were used, the single crystals for determinations of lattice parameters and ground-up bricks for powder intensity measurements.

Sodium  $\beta$  alumina was also made in our laboratory by heating together intimate pressed mixtures of sodium carbonate and  $\alpha$  alumina. Three compositions were used with  $\text{Na}_2\text{CO}_3:\text{Al}_2\text{O}_3$  ratios of 1:5, 1:6, and 1:11. The samples were annealed in air at 1200°C for 24 hours and then at about 1750°C for 20 minutes. The appearance of the samples after annealing at 1750°C shows that the reaction to give  $\beta$  alumina is very slow in the absence of a liquid phase. Whereas the two sodium rich samples had sintered to a hard mass, the sample poorest in sodium was still a fine powder. In addition, the x-ray pattern showed that whereas the former gave only  $\beta''$  alumina after firing at 1200°C and  $\beta$  alumina after firing at 1750°C, as expected from the phase diagram, the latter gave a mixture of  $\beta$  and  $\beta''$  alumina and  $\alpha$  alumina at both temperatures. This is what one would expect if there were inhomogeneities in the powder mixture and if the transport of material was restricted to slow solid state diffusion.

$\text{CaAl}_{12}^{0}{}_{19}$ , was made by the procedure outlined above. However, there was no x-ray evidence that reaction occurred during heating to 1200°C. On the other hand, annealing at 1750°C for about an hour produced the magnetoplumbite phase.

Other  $\beta$  aluminas were made by the cation exchange technique used by Yao and Kummer<sup>(17)</sup>. This involved immersing sodium  $\beta$  alumina in a molten salt, normally the nitrate of the cation that was desired to be exchanged for the sodium. Complete exchange was normally accomplished within a few hours. Where practical, metal M was also added to the melt to fix the activity of this species.

#### NEUTRON ACTIVATION ANALYSIS

Neutron activation analyses were performed upon sodium containing samples to evaluate their actual sodium content. The results for the polycrystalline samples made in this laboratory are presented in Table II-1.

Table II-1. Sodium Concentration (wt %) of Polycrystalline Samples

Composition <u>Na:Al</u>	Theoretical <u>Analysis</u>	Reacting Temperature	
		<u>1200°C</u>	<u>1750°C</u>
1:11	3.9	4.2	4.3
1:6	6.8	6.6	6.7
1:5	8.0	7.4	7.0

Crystals from large bricks of  $\beta$  alumina also showed 20-30% excess sodium over the concentration expected for  $\text{NaAl}_{11}^{0}{}_{17}$  and clear single crystals showed up to a 10% excess. It is felt that the accuracy of the neutron activation analyses may be no better than 5-10% so that the above numbers should only be used as a semi-quantitative guide to the sodium concentration.

## CHEMICAL AND SPECTROGRAPHIC ANALYSES

A clear single crystal of sodium  $\beta$  alumina was reacted to give silver  $\beta$  alumina. The reaction was then reversed and the silver concentration determined both by the weight change of the crystal and by the precipitation of the silver in the salt as chloride. These analyses indicated 97.5% and 98.9% respectively of the silver content expected for the stoichiometric formula  $\text{AgAl}_{11}^{0}_{17}$ .

Arc spectrographic analyses on a number of exchanged samples indicated that the main impurities were sodium and silicon 0.1 - 0.3 % in most cases.

## X-RAY ANALYSIS

A Picker x-ray diffractometer was used for all experiments, with Ni-filtered  $\text{CuK}_{\alpha}$  radiation. Single crystals were used for the determination of the c parameters and finely powdered samples for intensity measurements. Samples were powdered as finely as possible to eliminate the possibility of non-random orientation of the crystallites. This was particularly necessary because it was not possible to rotate the sample using this equipment. Intensity measurements quoted here are measured peak heights not peak areas.

The intensities of the diffraction lines expected for various test structures were calculated using the Stanford IBM computer. Incorporated into the program were the effects of multiplicity and angle on the intensity. In all cases the ionic positions within the  $\gamma$  blocks were assumed to be undistorted.

## RESULTS

### Magnetoplumbite Phase

Adelsköld <sup>(14)</sup> reported  $\text{CaAl}_{12}^{0}_{19}$  to have the same structure as magnetoplumbite. Since the bridging layers are close-packed there is little likelihood of it being grossly disordered. It was thus a good sample to test the methods to be used here. The agreement between

calculated and observed intensities was good. The lattice parameters were  $a_0 = 5.536$  and  $c_0 = 21.85$  Å. These compare favorably with those measured by Adelsköld,  $a_0 = 5.536$  and  $c_0 = 21.925$  Å.

The results obtained on this sample indicated that it was probably justifiable to assume no distortion of the  $\gamma$  blocks in structures of this type and that the techniques used here were satisfactory.

### $\beta$ Aluminas

#### 1) Sodium $\beta$ alumina

As can be seen from Plate II-1 there are insufficient ions in sodium  $\beta$  alumina to completely fill the bridging layers so there is the possibility of the ions residing on a variety of sites. The two types of sites considered by Beevers and Ross<sup>(2)</sup> are referred to as the normal and alternative sites; these are the sites at the center of the oxygen triangles. There are other possible sites for the sodium, such as midway between pairs of oxygen ions, but these are considered less likely candidates and will not be considered further here.

The results obtained here are given in Table II-2 along with those of Yamaguchi and Suzuki<sup>(7)</sup>. The calculated intensities for the normal and alternative sites are listed together with the calculated results of Yamaguchi and Suzuki for the normal site model. As can be readily seen, the agreement between observed and measured intensities is not very good, but it is readily apparent that the normal site model is far preferable to the alternative site model. This agrees with the conclusion of Beevers and Ross<sup>(2)</sup>.

In order to investigate whether the sodium ions might be distributed differently, several other possibilities were considered. A shortened version of the results is given in Table II-3, which includes a series of reflections whose intensities are markedly affected by the positions of the sodium ions. In addition to the previous models, the 3rd column of the calculated results is for a model in which 20% of the sodium ions have been placed on the alternative site. The 4th and 5th columns list the results assuming an excess of about 20% sodium in the bridging layer.

Table II-2

## X-Ray Intensities for Sodium Beta Alumina

hkl	<u>This Work</u>			<u>Yamaguchi and Suzuki</u> <sup>(7)</sup>		
	<u>Observed</u>	<u>Normal</u>	<u>Alternative</u>	<u>Normal</u>	<u>Observed</u>	<u>hkl</u>
002	69	100	100	100	120	002
004	38	22	22	24	51	004
100	-	1	-			
101	-	1	7			
102	11	9	-	11	7	102
103	8	3	9	3	6	103
106	3	-	-	-	1	106
008	18	3	3	3	6	008
107 } 110 }	39	22 10	16 10	28 13	44 8	107 110
114	26	22	22	29	23	{ 114 009
				-	4	108
200	-	2	-			
201	20	7	11	9	10	201
202	8	4	10	4	6	202
203	-	1	-	2	1	203
00.10	-	1	1	1	8	00.10
116	17	8	8	11	11	116
204	-	4	1	- 4	7	{ 109 204
205	17	13	10	14	15	205
10.10	-	2	-	-	6	00.11
206	23	14	9	17	15	206
				-	2	118
207	11	9	11	10	10	207
				-	1	10.11
208	4	3	6	4	5	208
				1	1	112
				-	2	123
				-	1	10.12
209	-	1	1	1 -	2	{ 209 214
20.10	2	2	4	3	2	20.10
300	-	2	2	2	6	300
00.14	-	1	1	2	6	00.14
217	15	10	7	7	10	217
20.11	11	9	7	12	11	20.11

In the first of these the excess charge is balanced by excess oxygen ions residing on the normal sodium site, the excess and displaced sodium residing on the alternative site. In the next column the excess sodium, which is assumed to reside on the alternative site, is balanced by aluminum vacancies in the bridging layer in a similar manner to that previously considered for both  $\beta'$  and  $\beta''$  alumina<sup>(7, 10)</sup>.

These calculations surely rule out the possibility that the sodium ions all reside on the alternative site but they cannot differentiate between the other two models.

Table II-3. X-Ray Intensities for 10 $\ell$  reflections of sodium  $\beta$  Alumina with Different Site Occupancy Models

hkl	Observed Intensity	Normal Site	Alt. Site	80% Norm. 20% Alt.	20% Excess Sodium	
					Na <sub>2</sub> O	A $\ell$ . Vac.
100	-	2	-	2	1	-
101	-	2	17	4	2	1
102	11	16	-	14	11	9
103	8	5	22	8	5	6
104	-	5	-	5	4	3
105	-	-	-	-	-	-
106	3	-	-	-	1	1
107	40	40	40	40	40	40

## 2) Thallium $\beta$ Alumina

The thallium ion plays a substantial role in the diffraction process in thallium  $\beta$  alumina and so its position in the crystal should be expected to have a profound effect on the intensities of the diffraction lines. In addition, the presence of light impurity ions, such as sodium and silicon, will have very little effect on the diffraction pattern because of the disparity in scattering power. The observed intensities of the more relevant lines for assigning the thallium positions are given in Table II-4,

together with the intensities calculated for a number of different thallium ion distributions. The designation of the models is the same as that used in the previous example.

Table II-4. X-Ray Intensities for Thallium  $\beta$  Alumina with Different Site Occupancy Models

hkl	Observed Intensity	Normal Site	Alt. Site	80% Norm. 20% Alt.	20% Exc. Na as Na <sub>2</sub> O	25% Exc. Na Na <sub>2</sub> O Al Vac.	
100	4	34	79	58	6	4	5
100	100	100	6	100	100	100	100
102	4	83	100	100	25	6	2
103	48	56	8	58	55	53	53
104	6	44	72	63	11	-	2
105	71	50	1	50	51	47	50
106	12	10	67	35	-	4	8
107	(very large)	(very large)	14	(very large)	(very large)	(very large)	(very large)
108	12	3	47	18	1	2	9
109	12	13	1	14	13	12	12
1010	-	13	10	17	4	3	-
1011	36	11	-	11	11	15	12

The results indicate clearly that the best agreement is found if a 25% excess of thallium is assumed. This is in agreement with the activation analysis of the sodium content of the material from which these samples were prepared. However, from these results alone, one is not able to differentiate between the two proposed models for balancing the net positive charge due to the presence of excess sodium.

### 3) Other $\beta$ Aluminas

Samples of lithium, ammonium, and potassium  $\beta$  alumina all gave diffraction patterns consistent with the  $\beta$  alumina structure. Only in the case of the potassium compound was the ion heavy enough to show definite evidence for a

25% excess of alkali metal.

The x-ray pattern of silver  $\beta$  alumina could also best be explained by assuming about a 25% excess of silver. However the agreement between observed and calculated intensities was much poorer than for the thallium compound. This may be because the silver ion is far more covalent in its bonding than the other ions considered here and thus will have a greater tendency to distort the surrounding oxygen layers and also to find other sites in order to enhance the covalent nature of its bonding with the oxygens. Powder samples of silver  $\beta$  alumina also had an anomalously small  $c$  parameter for the size of the silver ion relative to the other  $\beta$  aluminas investigated, see Figure II-2.

#### THE SODIUM RICH PHASE (SODIUM $\beta''$ ALUMINA)

The  $d$  spacings and the intensities of the reflections of two samples with overall compositions  $\text{Na}_2\text{O}:5\text{Al}_2\text{O}_3$  and  $\text{Na}_2\text{O}:6\text{Al}_2\text{O}_3$ , together with those of They and Briancon<sup>(3)</sup> are given in Table II-5. The closeness of the results tends to indicate that the phases are the same; the discrepancies in the  $d$  values at low angles is probably due to errors in diffractometer alignment. The lattice parameters of this phase as determined by various investigators are given in Table II-6. Only the data of Bettman and Peters are for single crystals.

Table II-6.

Lattice Parameters for Sodium  $\beta''$  Alumina

<u><math>a_0</math></u>	<u><math>c_0</math></u>	<u>Investigator</u>
5.61	33.95	They and Briancon <sup>(4)</sup>
5.595	33.93	Yamaguchi and Suzuki <sup>(8)</sup>
5.614	33.85	Bettman and Peters <sup>(11)</sup>
5.611	33.88	This Work

Inspection of the data of Table II-5 shows that they can be indexed assuming a  $c$  axis repeat distance of one-third the cell length. As this distance is almost identical to the repeat distance in  $\beta$  alumina, it

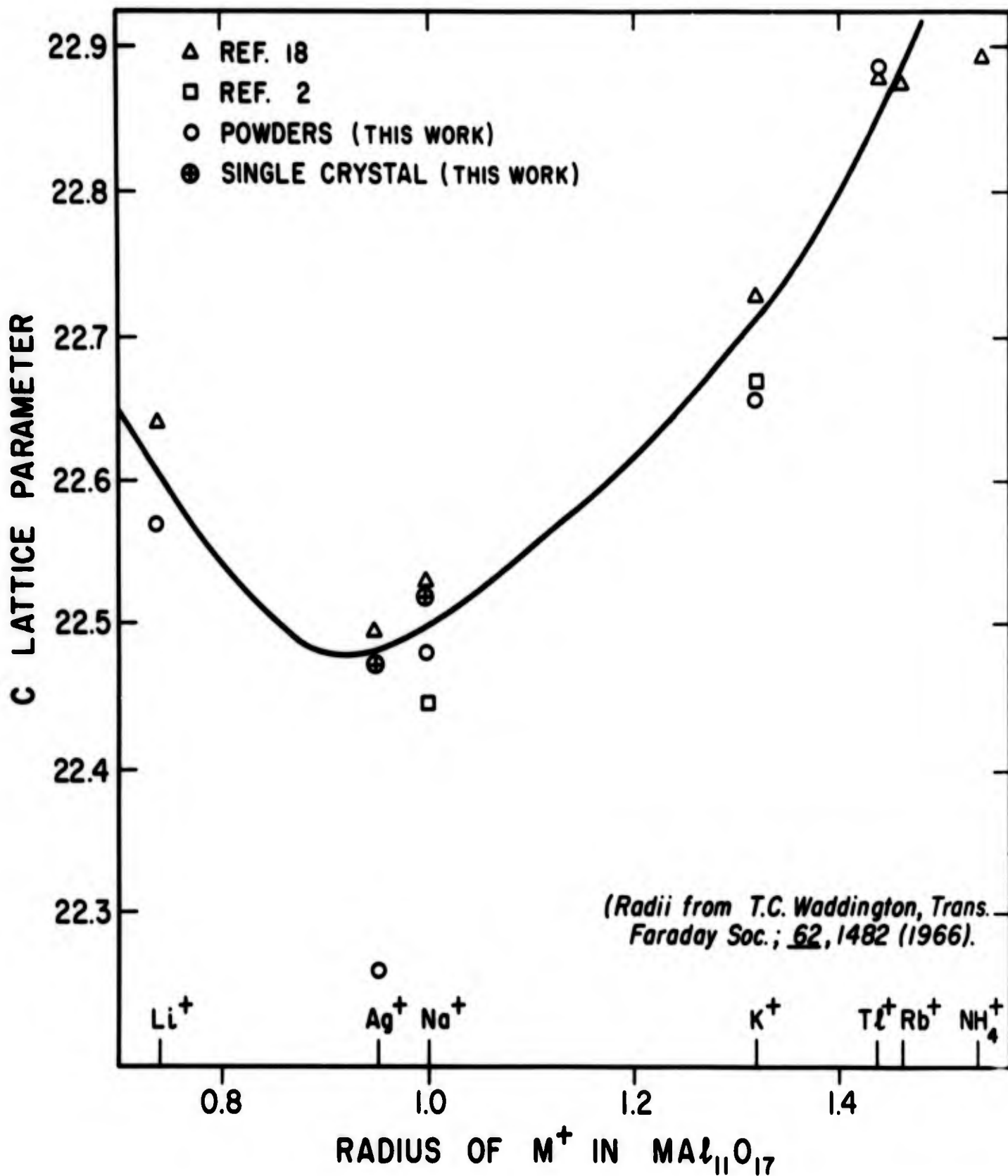


Figure II-2 Lattice Parameter,  $C_o$ , of  $MA_{11}O_{17}$ .

Table II-5. X-Ray Data From Sodium Rich Phase

hkl	This Work					Thery and Briancon <sup>(3)</sup>			
	calc.d	Na <sub>2</sub> Al <sub>12</sub> O <sub>19</sub>			NaAl <sub>5</sub> O <sub>8</sub>		NaAl <sub>5</sub> O <sub>8</sub>		hkl
		d	I	d	I	d	I		
003	11.30	11.19	67	11.5	38	11.55	VS	003	
006	5.65	5.63	34	5.70	25	5.69	S	006	
102	4.67	4.67	3.5	4.7	4	3.71	VW	102	
103	4.46	4.44	2	4.5	1	-	-	-	
104	4.22	4.22	10	4.24	8	4.24	W	104, 008	
		2.940	2						
110	2.805	2.804	23	2.81	22	2.808	MS	110	
10.10	2.771	2.778	15	2.78	8	2.801	M	111	
113	2.723	2.679	6	2.69	4	2.666	VW	114	
10.11	2.602	2.600	21	2.61	20	2.609	MS	10.11, 0013	
116	2.512	2.510	34	2.52	30	2.518	S	116	
201	2.422	2.423	15	2.425	14	2.424	M	200, 0014, 117	
203	2.375	2.374	2		-	2.380	VW	203	
204	2.335	2.337	16	2.340	15	2.337	M	204, 118	
205	2.287	2.287	4	2.29	3	2.289	VW	205	
119	2.250	2.249	17	2.25	12	2.253	M	119	
207	2.171	2.168	8	2.17	7	2.173	W	207, 10.14	
-	-	2.137	3	2.145	2	-	W	-	
208	2.107	2.103	1		-		-		
209	2.041	2.036	3	2.04	2	2.040	W	209	
20.10	1.974	1.973	35	1.975	34	1.976	VS	20.10	
10.16	1.941	1.937	3	1.944	3	1.940	VW	10.16	
20.10	1.615	1.614	6	1.62	7	1.616	W	300, 301, 21.10	
20.16	1.596	1.595	8	1.60	8	1.598	MW	20.16	
21.11	1.577	1.578	8	1.58	8	1.577	MW	21.11	
306	1.557	1.556	6	1.56	5	1.555	W	306	
20.17	1.541	1.540	3	1.54	3	1.540	VW	21.12, 10.21	
309	1.488	1.486	4	1.49	4	1.486	VW	309	
21.14	1.463	1.463	1.5	1.46	2	1.462	VW	30.10, 21.14	
20.19	1.438	1.437	2	1.44	1	1.436	VW	20.19, 30.11	
		Small peak on edge of large one				1.43	VVW	00.24	
220	1.403	1.403	31	1.403	28	1.401	MS	220	
223	1.392	1.389	18	1.392	17	1.390	M	223	
226	1.365	1.361	4	1.365	4	-	VW	-	

Table II-5. (continued)

NOTE: The indexing here is by no means exhaustive. It is merely a temporary assignment to show that the lines can be indexed using the condition that when  $h = k$ ,  $l$  must be  $3 \times n$ . The correct indexing can only be achieved when the structure is fully known. The intensities of They's and Briancon's compound were read from the figure in their paper using the standard approximations for the intensities of the lines, i.e., strong, medium, and weak, and combinations of these.

---

seems reasonable to assume that the structure is made up of three of the blocks of the  $\beta$  alumina structure. If these have essentially the same arrangement one would expect reflections where  $h = k$  and  $l$  is not  $3 \times n$  to be missing. An attempt was made to so index our x-ray pattern; the result is shown in Table II-5. With few exceptions it was found possible; all the exceptions were of weak intensity.

Test structures were thus based on a model comprising three  $\gamma$  blocks separated from one another by bridging layers as in  $\beta$  alumina. As discussed earlier there are 9 Al and 16 O in the  $\gamma$  block so there must be 2 Na and 1 Al, and 2 Na, 3 Al and 3 O for  $\text{NaAl}_5\text{O}_8$  and  $\text{Na}_2\text{Al}_{12}\text{O}_{19}$  respectively in the bridging layer. Inspection of structures of the  $\beta$  alumina type shows that only four large ions, i.e., non-aluminum ions, can be fitted into the bridging layers. The actual composition of the  $\beta''$  alumina phase must be somewhere between the two formulas given above as the structure is unlikely to be stable in the absence of oxygen ions in the bridging layers, as is required by the formula  $\text{NaAl}_5\text{O}_8$ , and the lattice cannot contain all the ions required for the formula  $\text{Na}_2\text{Al}_{12}\text{O}_{19}$ .

In the building of any model two different aspects of the structure must be considered, the arrangement of the  $\gamma$  blocks relative to one another and the arrangement of the ions within the bridging layers. Either of these can be the cause for there being three  $\gamma$  blocks in the unit cell. To simplify the model building it would be very convenient to have ions in the bridging layer which provide a negligible contribution to the total x-ray scattering so that these layers can in a first approximation be neglected. After the ionic positions in the rest of the lattice have been determined then the ionic positions in these layers can be accurately ascertained using a heavy atom such as thallium in the place of sodium. Ideally the lithium compound would be better to study than the sodium analog, but  $\text{LiAl}_5\text{O}_8$  has the spinel structure. As the ions in the bridging layer will provide some contribution to the total scattering, the intensities of weak lines may be markedly changed by ignoring these layers. However, strong reflections are not likely to be changed appreciably. So the first goal of this work was to get reasonable agreement with the strong reflections.

As in the case of the  $\beta$  alumina structure, certain series of reflections are expected to be more sensitive to the ionic arrangements than

others. Thus, lines of the type 001 may be rather insensitive, whereas those of the type hkl where  $h \neq k$  might be expected to be more sensitive. As the most prominent reflection of this phase is the 20.10 line, emphasis was placed on the 20l series of lines. This series has another interesting characteristic, the reflections  $20.3n + 1$  are the most intense. The intensities of these lines are tabulated in Table II-7 for compositions with  $\text{Na}_2\text{O}:\text{Al}_2\text{O}_3$  of 1:5 and 1:6.

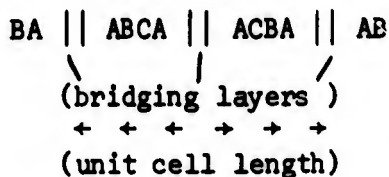
Table II-7. Observed Intensities for the 20l Lines of the  $\beta''$  Phase

hkl	$\text{Na}_2\text{O}:\text{Al}_2\text{O}_3$	
	1:6	1:5
200	-	-
201	15	14
202	-	-
203	2	-
204	16	15
205	4	3
206	-	-
207	8	7
208	1	-
209	3	2
2010	35	34
2016	8	8

Considering the difference in the composition, the intensities are remarkably similar. This may be indicative of this phase having a narrow composition range, the excess components being present as a second phase too low in concentration to be detected by x-ray analysis.

Initial work showed that the arrangement of the  $\gamma$  blocks relative to one another had a marked effect on the relative intensities of the 20l series of reflections. In  $\gamma$  alumina the oxygen ions are cubic close-packed so that only in every fourth layer are the oxygens in the same position, in contrast to  $\alpha$  alumina where every third layer is the same. Thus, if the three different close-packed layers are described by the letters A, B, and

C, the arrangement in  $\beta$  alumina is given by



In the sodium rich phase there are three  $\gamma$  alumina blocks separated from one another by bridging layers. There are a number of ways in which these blocks may be arranged. In the simplest case the blocks may simply repeat one another, as in (a) Table II-8. In model (b) short range mirror planes are introduced to give a greater resemblance to  $\beta$  alumina. Model (c) is based on the insertion of the bridging layers after every fourth oxygen layer in a cubic close-packed lattice, and model (d) assumes the replacement of every fifth layer of a cubic close-packed lattice with the bridging layer.

---

Table II-8. Possible Stacking Models for the Sodium Rich Phase

(a)	CA    ABCA    ABCA    ABCA    AB
(b)	CA    ABCA    ACBA    ABCA    AB
(c)	BC    ABCA    BCAB    CABC    BA
(d)	AB    ABCA    CABC    BCAB    AB

← (unit cell length) →

---

The results of computer calculations for each of these four models are compared with the experimental data in Table II-9. It is quite apparent that model (d) gives a much better fit to the observed data than the other three. To refine this model one oxygen and two aluminum ions were added to the bridging layers in the same position relative to the ions in the  $\gamma$  block as those three ions have in the  $\beta$  alumina structure. The results of calculations based on this refinement are given in Column (e). These results bear a very close resemblance to the observed intensities. The complete results are given in Table II-10. There are five lines that cannot

Table II-9. Comparison of Intensities for  $\gamma$  Block Stacking Models in Sodium  $\beta''$  Alumina

<u>hkl</u>	<u>Stacking Model</u>					<u>Observed</u>
	(a)	(b)	(c)	(d)	(e)	
200						44
201				6	27	
202			31			-
203	44	50				6
204				46	36	46
205			34	9	15	10
206	8					-
207				9	14	23
208		18	70	1	4	3
209	100	100				7
2010		30		100	100	100
2011		24	100			-

be accounted for by this structure. However, these lines, marked \* in the Table, can be assigned to the 102, 106, 202, 205, and 206 reflections of the  $\beta$  alumina phase. It, thus, appears that there must have been a small amount of this second phase present both in This work and in that of They and Briancon<sup>(3)</sup>. Bettman and Peters<sup>(10)</sup> reported that this compound has the higher rhombohedral symmetry. Rhombohedral indexing is also given in Table II-10, and it can be seen that all but the five lines mentioned above also can be indexed according to this symmetry. The parameters of this cell are  $a_0 = 11.750 \text{ \AA}$  and  $\alpha = 27^\circ 37'$ .

It now merely remains to find the best position for the sodium ions. In this structure each bridging layer contains two equivalent tetrahedral vacancies or three equivalent octahedral vacancies where the ions could reside. As the sodium ions only weakly scatter x-rays it will be necessary to use a heavy ion instead to determine the occupied positions unequivocally. The thallium analog is presently being studied for this purpose.

Table II-10. Results for the Sodium Rich Phase.

<u>hkl</u>	<u>Hexagonal</u>				<u>Rhombohedral</u>
	<u>meas. d</u>	<u>calc. d</u>	<u>meas. I</u>	<u>calc. I</u>	<u>hkl</u>
003	11.37	11.30	150	500	111
006	5.67	5.65	86	110	222
012	4.69	4.67	10	24	110
103 *	4.46	4.46	4	-	
104	4.23	4.22	26	26	211
*	2.940		3	-	
110	2.806	2.805	66	23	10 $\bar{1}$
10.10	2.779	2.779	34	29	433
113	2.685	2.723	15	1	210
01.11	2.605	2.602	60	35	443
116	2.515	2.512	93	54	321
021	2.424	2.423	43	27	11 $\bar{1}$
203 *	2.374	2.375	3	-	
024	2.338	2.335	45	35	220
205	2.288	2.287	10	16	311
119	2.250	2.250	43	43	432
027 } 01.14 }	2.169	2.171 2.167	22	{ 13 8	331 554
*	2.141		7	-	
208	2.103	2.107	2	4	432
209 *	2.038	2.041	7	-	
02.10	1.974	1.974	100	100	442
10.16	1.940	1.941	9	3	655
300 } 21.10 }	1.617	1.620 1.615	19	{ 4 13	11 $\bar{2}$ 532
01.20	1.598	1.600	23	4	776
02.16		1.596		22	664
12.11	1.578	1.577	23	17	542
306	1.556	1.557	16	11	330
20.17	1.540	1.541	9	10	755
309	1.486	1.488	12	13	441
12.14	1.463	1.463	4	4	653
02.19	1.437	1.438	4	5	775
220	1.403	1.403	86	63	20 $\bar{2}$
223	1.390	1.392	51	8	31 $\bar{1}$
226	1.363	1.361	12	7	420

## DISCUSSION AND CONCLUSIONS

The results obtained here on powdered samples of  $\beta$  alumina indicate that these samples tend to have an excess of the cation M relative to the stoichiometric formula,  $MA_{11}O_{17}$ . This excess metal ion resides on the alternative site in the bridging layer, the normal site being completely occupied. There was no evidence for the metal ions favoring the alternative site to the normal site. This work was unable to differentiate between the two models, considered for balancing the electrostatic charge of the excess M, excess oxygen ions, or aluminum vacancies. Neither model is particularly satisfactory from an electrostatic energy standpoint. In the former, the excess oxygen ions are surrounded by six other oxygen ions, and in the latter the removal of a triply charged small ion will require a lot of energy and will leave an oxygen ion with other oxygen ions as nearest neighbors. Techniques other than structural will be required to determine the type of defects present.

The available experimental evidence indicates that there is only one sodium rich phase with a composition  $Na_2O:Al_2O_3$  somewhere between 1:5 and 1:6. The structure is very similar to that of  $\beta$  alumina, the main difference being that there are three  $\gamma$  blocks per unit cell in place of the two of  $\beta$  alumina. The three blocks are related by a three-fold screw axis whereas the two in  $\beta$  alumina are related by a two-fold screw axis. As a result of this, sodium  $\beta''$  alumina exhibits rhombohedral symmetry. The structure found here for this phase is the same as that found recently by Bettman and Peters<sup>(10)</sup> and by Yamaguchi and Suzuki<sup>(8)</sup>. Both these teams of workers suggested that the sodium ions occupy the tetrahedral sites in the bridging layers, which would give a maximum sodium content double that of sodium  $\beta$  alumina. They considered the sodium charge excess over that of 3 Na per unit cell to be balanced by aluminum vacancies in the same way as considered for the excess sodium in  $\beta$  alumina above. We do not think that our data are sufficiently reliable to differentiate between the different sites available for the sodium or between the two possible mechanisms of charge compensation.

The sodium  $\beta'$  alumina phase reported by Yamaguchi and Suzuki<sup>(7)</sup>, which only differs from the  $\beta$  alumina structure in the positions of the sodium ions, seems most probably to be just a stoichiometric variation of  $\beta$  alumina and not a separate phase.

#### ACKNOWLEDGEMENTS

The authors wish to acknowledge helpful discussions with Max Bettman of the Ford Motor Company and Walter Roth of the General Electric Research and Development Center in addition to R. W. Helliwell and W. D. Nix of Stanford University. G. W. Martin of the Center for Materials Research at Stanford (supported by the Advanced Research Projects Agency) was of considerable assistance with the x-ray studies. Thanks are also due to The Carborundum Company for contributing samples of sodium  $\beta$  alumina.

## REFERENCES

1. C. A. Beevers and S. Brohult, Z. Krist. 95, 472 (1936).
2. C. A. Beevers and M. A. S. Ross, Z. Krist. 97, 59 (1937).
3. J. Thery and D. Briancon, Rev. Hautes Temp. Refract. 1, 221 (1964).
4. J. Thery and D. Briancon, Comptes Rendus 254, 2782 (1962).
5. R. Scholder and M. Mansmann, Z. Anorg. Allgem. Chem. 321, 246 (1963).
6. M. Rolin and P. H. Thanh, Rev. Hautes Temp. Refract. 2, 175 (1965).
7. G. Yamaguchi and K. Suzuki, Bull. Chem. Soc. Jap. 41, 93 (1968).
8. E. Kordes, Z. Krist. 91, 193 (1935).
9. J. Felsche, Z. Krist. 127, 94 (1968).
10. M. Bettman and C. R. Peters, to be published in J. Phys. Chem.
11. S. Wallmark and A. Westgren, Arkiv Kemi 12B, No. 35 (1937).
12. K. Lagerquist, S. Wallmark, and A. Westgren, Z. Allgem. Chem. 234, 1 (1937).
13. R. Blix, Geol. Foren. Forhand, Stockholm 59, 300 (1937).
14. V. Adelsköld, Arkiv Kemi 12A, No. 29 (1938).
15. G. Yamaguchi, Elect. Chem. Soc. Jap. 11, 260 (1943).
16. P. Braun, Philips Research Reports 12, 691 (1957).
17. Y. Y. Yao and J. T. Kummer, J. Inorg. Nucl. Chem. 29, 2453 (1967).

CHAPTER III

DEFECT EQUILIBRIA IN BETA ALUMINA AND

RELATED PHASES

M.S. WHITTINGHAM

R.W. HELLIWELL

R.A. HUGGINS

## INTRODUCTION

In order to guide the exploratory portion of this program and to provide a theoretical framework to help understand the wide variety of experimental observations of defect-related properties, some attention has been given to the development of an appropriate model to describe defects in systems of the  $\beta$  alumina type. Any realistic model must be consistent with and quantitatively amenable to treatment in terms of the general quasi-chemical approach that has been developed for the thermodynamic description of defects in other related, although structurally simpler, materials.

This chapter summarizes the results of the examination of the thermodynamic consequences of several possible disorder types. In addition, the influence of experimental conditions and previous sample history upon the predominant defect types and their concentrations will be discussed, since these are the important factors determining the properties of ionic conductors as electrochemical transducers.

## GENERAL COMMENTS RELATING TO PHASE EQUILIBRIA IN RELEVANT TERNARY SYSTEMS

The Gibbs Phase Rule indicates that if, in addition to the hydrostatic pressure and temperature, two other independent variables are specified in a ternary system, the number of degrees of freedom under equilibrium conditions goes to zero, and the system is completely determined. In structural terms, this means that if equilibrium is attained (even locally) the identity of all the defects present and their respective concentrations will be fixed. Furthermore, because of the relationship between defect concentrations and overall chemical composition, the latter will also be determined. Conversely, if the chemical composition is accurately known, all the pertinent defect concentrations and thermodynamic quantities are specified.

The compositions of ternary phases are often illustrated by the use of the familiar Gibbs triangle with the pure components at the three corners. Assuming a general ternary system M-N-O, the  $\beta$  alumina phase and the other phases pertinent to this discussion nominally lie along a line (sometimes

called a pseudo-binary line) connecting the points along the periphery representing compositions having the stoichiometric ratios and chemical formulas  $M_2O$  and  $N_2O_3$ . Points representing compositions with several specific ratios of the end compositions are shown in Figure III-1. For example,  $\beta$  alumina is normally described as having a nominal composition ratio of 1:11. The various values of this composition ratio reported for the phases in this system are discussed in detail in another chapter, and will not be included here.

Because of the entropy change accompanying the presence of defects, all phases must, in principle, be stable over a range of composition at any given temperature above 0°K. This range usually, but not necessarily, encompasses the nominal or stoichiometric composition.

A schematic isothermal Gibbs triangle in which rather wide compositional ranges are assumed for the relevant phases is shown in Figure III-2. It should be recognized that a number of other assumptions have also been made in drawing that figure for illustrative purposes.

An expanded version of part of the hypothetical Gibbs triangle is shown in Figure III-3. Looking specifically at the  $\beta$  phase, the line a-b represents the maximum limit of the stable composition range with respect to oxygen. Compositions along that line are in equilibrium with oxygen at a given value of oxygen activity (partial pressure). Likewise, points along the line a-e represent compositions in equilibrium with  $\beta''$ , and those along line d-e are in equilibrium with the practically pure M solid solution. Every point within a single phase region represents a unique composition ratio of M:N:O, and also can be described by a unique set of activity values.

Since two of the boundaries, lines a-e and d-e, of the  $\beta$  alumina phase field represent compositions at which the activity of M  $\beta''$  alumina and of metal M itself are essentially equal to unity, point e, where these two lines converge, is determined by the oxygen activity at which the metal and oxide are in equilibrium. As the temperature changes, the oxygen activity for this equilibrium will also vary. This oxygen activity goes up with temperature in all common metal-metal oxide systems, as may be readily seen by inspecting the common Ellingham diagram. At higher temperatures the phase field extends

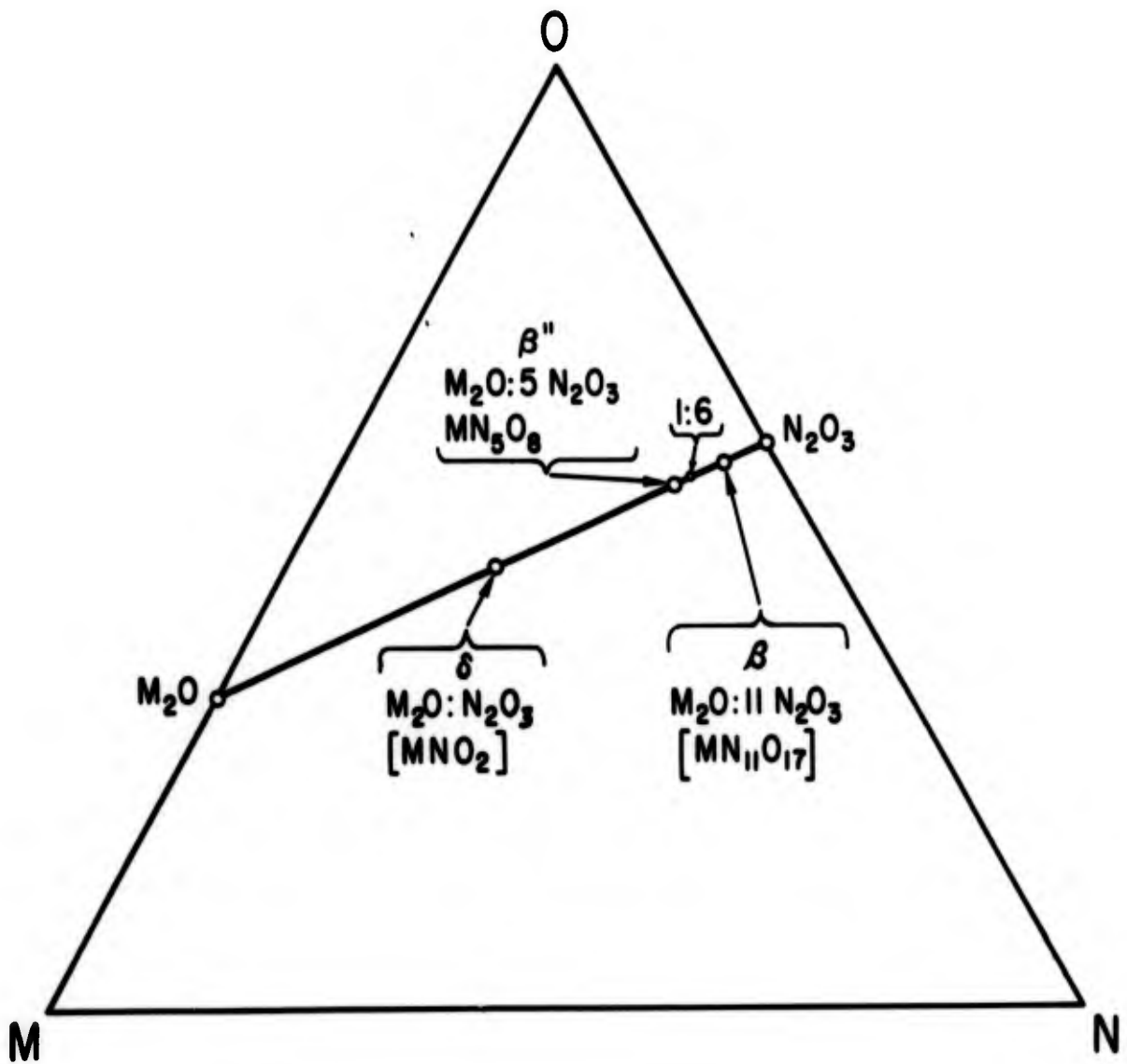


Figure III-1 Gibbs triangle for system M-N-O showing normal compositions for beta alumina and several related phases.

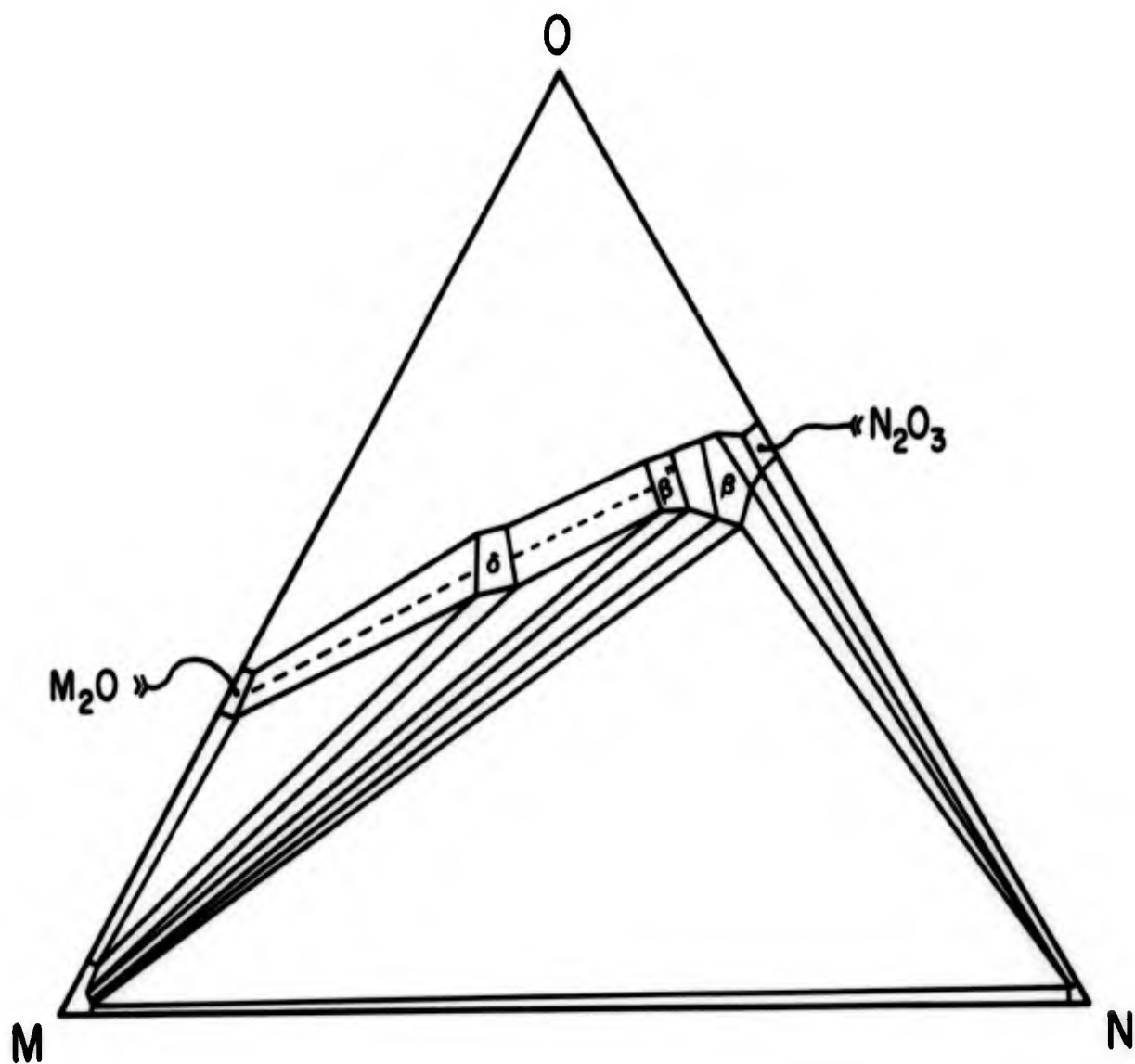


Figure III-2 Hypothetical isothermal Gibbs triangle for system M-N-O showing composition ranges for several phases.

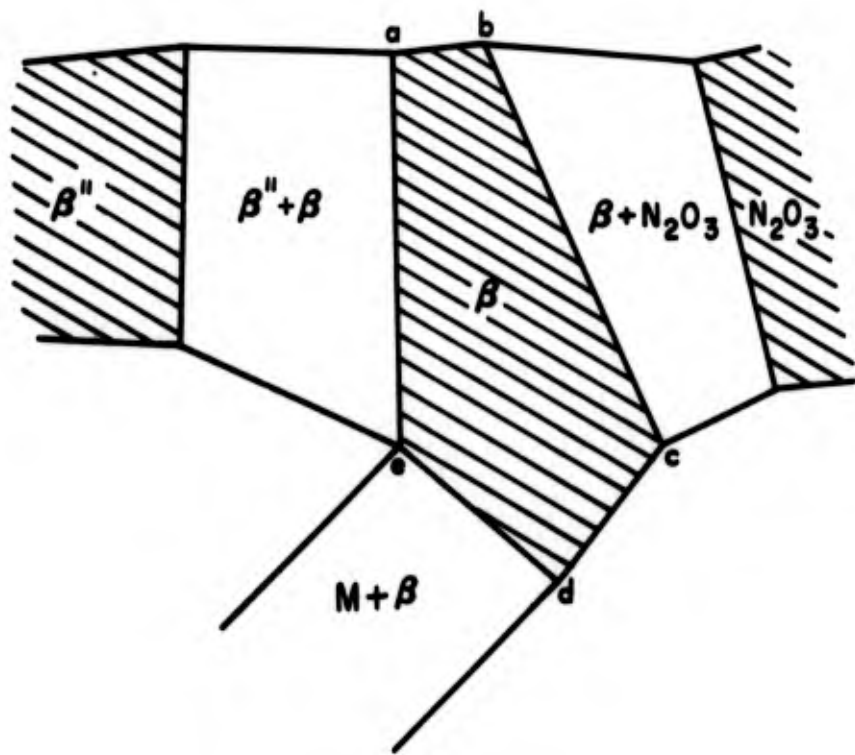
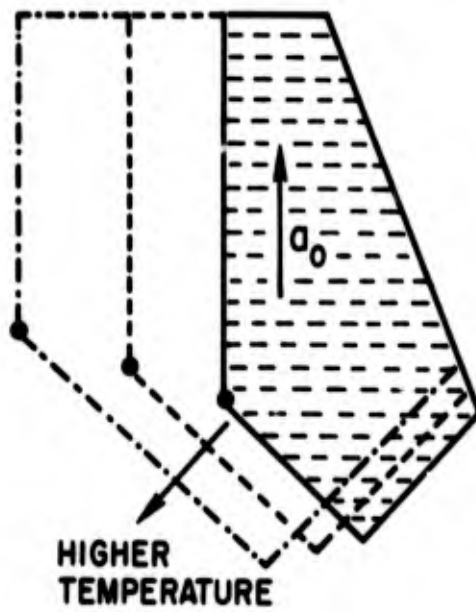


Figure III-3 Expanded portion of isothermal Gibbs triangle.

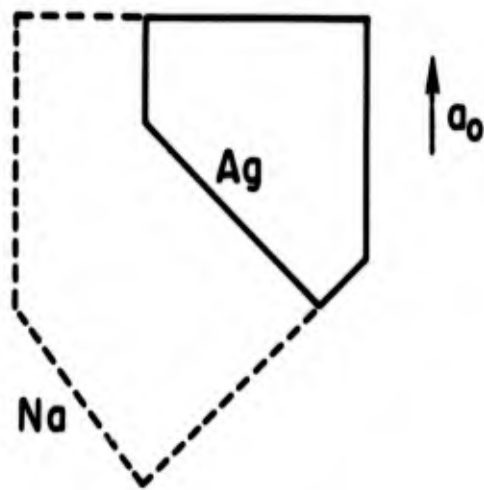
further to the left and also toward component M as point e moves to greater oxygen activities as shown in Figure III-4a.

A second consideration is the effect on the extent and shape of the phase field of the identity of metal M. The more stable the M oxide, the lower the oxygen activity at which the lines a-e and d-e meet. In addition, the greater the stability of the M-O bond the greater the breadth of the phase field to the left. This is schematically illustrated in Figure III-4b for  $\beta$  alumina containing sodium and silver, two extreme cases. The result is that a sample equilibrated at any given temperature with sodium is going to have a higher solubility of M than would be possible in the equivalent silver case. This also means that if all the sodium ions were to then be replaced by silver ions the sample would be super saturated. Furthermore, since the equilibrium oxygen activity for the formation of these two oxides is quite different, the super saturation will be with respect to silver metal rather than to silver oxide. For those oxides, e.g., thallium and copper, whose free energy of formation falls between these two extremes, conditions should occur where either the oxide or the metal may precipitate.

In accordance with the phase rule, the specification of two independent compositional variables defines any point within a given single phase field. Instead of using two compositional relations directly, it is often more convenient to specify the position of the point in terms of the values of two activities. In oxide systems the activity of oxygen is an obvious choice. There are two reasonable alternatives for the second choice, the value of the activity of either M or N, or the activity of the terminal phase on the pseudo-binary line. The latter was used by Schmalzried and Wagner<sup>(1,2)</sup> in their important papers on defects in ternary phases. In order to see how these approaches are really equivalent, consider Figure III-5. Any point can be described by the intersection of a pair of isoactivity lines in either case. The values of the various activities are, of course, interrelated by the integrated form of the Gibbs-Duhem equation. Because of the unique structure of  $\beta$  alumina phases which results in an unusually large difference in the mobilities of the different structural species, as well as the presence of more than one intermediate phase in the pseudo-binary system, it seems more appropriate to use the activities of the cation M and of oxygen as the independent variables in this work.



a.



b.

Figure III-4 Schematic illustration of effect of temperature and identity of metal M on left hand portion of the phase field of beta alumina.

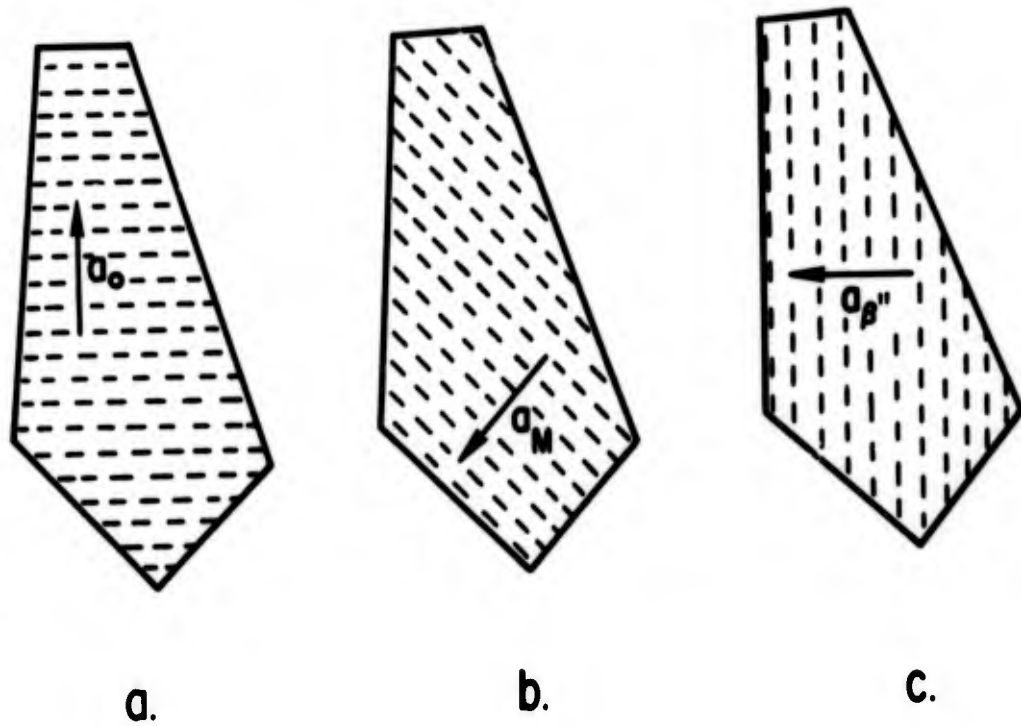


Figure III-5 a) Oxygen isoactivity lines shown schematically in beta phase field  
 b) M isoactivity lines  
 c)  $\beta''$  isoactivity lines

The next section of this chapter will present a general method to be used to relate the defect structure and chemical composition of a ternary phase to the values of these two parameters.

#### USE OF THE QUASI-CHEMICAL REACTION APPROACH FOR THE CALCULATION OF DEFECT EQUILIBRIA IN TERNARY SYSTEMS

A general method for the determination of the defect equilibria in solids based upon the treatment of defects as chemical species and the use of quasi-chemical reactions between them and external species has recently been described for a number of simple cases elsewhere<sup>(3,4,5)</sup>.

The first step in this method is to postulate the identity of the major defect species present, including electrons and holes. A system containing  $n$  different types of defects can be solved by writing  $(n-1)$  mass action equations, relating to different quasi-chemical reaction equilibria, as well as the electroneutrality condition. Simultaneous solution of these  $n$  equations in  $n$  unknowns is simplified by writing the mass action equations in logarithmic form so that they become linear and by making appropriate approximations to the electroneutrality condition.

In general, it is reasonable to expect to consider four predominant defects in materials composed of species with a strong preference for a single value of valence. Two of these defects are generally electron and holes the others are crystallographic defects. If one of the defects can be present with two different values of relative electrostatic charge, they are treated as separate species, and another mass action relation is needed, relating to the corresponding ionization reaction. Likewise, if the same chemical species can reside in crystallographically different imperfection sites it is formally treated as though two different species were present.

In the case of binary systems with four predominant defects, the pertinent quasi-chemical equilibrium reactions normally involved are:

- 1) the formation of an electronic defect pair (electron and hole),
- 2) the formation of a pair of crystallographic defects, and
- 3) the interaction between defect species within the solid and species in an adjacent phase (such as oxygen in the atmosphere).

This last relation constitutes the specification of an independent thermodynamic variable and so the thermodynamic state of the system is determined.

In ternary systems, on the other hand, two independent thermodynamic variables must be specified. Therefore, one additional compositional relation is needed. However, the total number of equilibria is not changed, for no simple equilibrium relation for the formation of a simple pair of crystallographic defects can be written in ternary systems without the introduction of another chemical species because of the requirements for crystallographic site balance. As a result, in addition to the electro-neutrality condition, the pertinent relations in ternary systems are generally

- 1) the mass action equation for the electronic defect pair formation reaction,
- 2) the mass action equation for equilibrium between some pair of defect species within the solid and an electrically neutral component in an adjacent phase, and
- 3) some other compositional relation, such as the specification of the concentration of one defect species, the concentration or activity of a component, or the ratio between such measures of two species or components.

After an appropriate set of simultaneous equations has been selected they can be solved to give the concentrations of all defect species as a function of the prescribed thermodynamic (compositional) variables. The results are often presented in the form of Defect Equilibrium Diagrams, one form of which shows the defect concentrations (plotted on a logarithmic scale) versus the value of the activity of the component referred to in 2) above. In oxides this is normally the oxygen activity (or partial pressure). The desirability of the use of the logarithmic form of the mass action expressions as well as a simplified way of presenting this information that emphasizes the approximations made on the electroneutrality condition were first pointed out by Brouwer<sup>(6)</sup>. Specific examples will be presented later.

## DEFECT EQUILIBRIA IN PHASES OF THE BETA ALUMINA TYPE

Information concerning the overall composition and structure of  $\beta$  alumina and the related sodium rich phase described in another chapter of this report can be used to predict the most probable types of disorder in such materials.

In both phases the structure is described in terms of parallel blocks or sheets having aluminum ions (comparable to N in the previous discussion) and oxygen ions in the  $\gamma$  alumina structure. These sheets are joined or bridged by monolayers containing monovalent (M) cations and oxygen ions in Al-O-Al bridging groups. It is assumed that all of these ions carry their common ionic charges.

Because of the much greater ionic mobility expected in the bridging layers than in the  $\gamma$  blocks, it is reasonable to expect that compositional and defect equilibria can be achieved selectively in such materials. That is, changes in the  $\gamma$  blocks are not to be expected except at high temperatures, whereas local equilibrium should be readily attained at much lower temperatures in the bridging layers.

The structural information presented in another chapter of this report leads to the postulation of a relatively small number of possible disorder types in these materials, which are assumed to be primarily ionic conductors in accordance with other information reported elsewhere.

The following disorder types will be considered:\*

- 1)  $M_i^\circ$  and  $O_i''$  (type of anti-Schottky disorder)

(this seems most consistent with the excess  $M_2O$  concentration reported in  $\beta$  alumina)

- 2)  $V_M'$  and  $V_O^{\circ\circ}$  (type of Schottky disorder)

(this may be more important in  $\beta''$  phase)

- 3)  $M_i^\circ$  and  $V_{Al}'''$  (type of Frenkel disorder)

(this was suggested by structural studies of Yamaguchi and Suzuki, and Bettman and Peters for  $\beta''$  phase)

\* The defect notation used is essentially that used in reference 3.

As discussed above there are a number of pertinent relations for a ternary system.

a) a law of mass action expression for electron-hole pair formation:

$$K_e = [e'] [h^\circ] \quad (1)$$

b) laws of mass action relations reporting the reaction between an external species and a pair of defects within the solid, one crystallographic and the other electronic. Relevant examples are:

<u>Defect</u>	<u>Quasi-chemical Reaction</u>	<u>Law of Mass Action Equation</u>	
$O_i''$	$1/2 O_2 \rightleftharpoons O_i'' + 2 h^\circ$	$K_o = \frac{[O_i''] [h^\circ]^2}{p_{O_2}}$	(2)

$V_O^{\circ\circ}$	$O_O \rightleftharpoons 1/2 O_2 + V_O^{\circ\circ} + 2e'$	$K_o' = [V_O^{\circ\circ}] [e']^2 p_{O_2}^{1/2}$	(3)
--------------------	---	--	-----

$M_i^\circ$	$M \rightleftharpoons M_i^\circ + e'$	$K_M = \frac{[M_i^\circ] [e']}{a_M}$	(4)
-------------	---------------------------------------	--------------------------------------	-----

$V_M'$	$M_M \rightleftharpoons M + V_M' + h^\circ$	$K_M' = [V_M'] [h^\circ] a_M$	(5)
--------	---	-------------------------------	-----

$V_{Al}'''$	$Al_{Al} \rightleftharpoons Al + V_{Al}''' + 3 h^\circ$	$K_{Al} = a_{Al} [V_{Al}'''] [h^\circ]^3$	(6)
-------------	---	---	-----

In each case the law of mass action expression is written in terms of defect concentration, but in terms of the activities of the components in the external phase.

c) an equation can be set up relating the activities of the three components from the formation reaction:

$$MA_{11}O_{17} \rightleftharpoons M + 11 Al + 17/2 O_2 \quad K_a = a_{Al}^{11} p_{O_2}^{17/2} a_M \quad (7)$$

The above equations may be more usefully written in logarithmic form:

$$\ln K_e = \ln [e'] + \ln [h^\circ] \quad (8)$$

$$\ln K_O = \ln [O_i''] + 2 \ln [h^\circ] - 1/2 \ln p_{O_2} \quad (9)$$

$$\ln K_O' = \ln [V_O^{\circ\circ}] + 2 \ln [e'] + 1/2 \ln p_{O_2} \quad (10)$$

$$\ln K_M = \ln [M_i^\circ] + \ln [e'] - \ln a_M \quad (11)$$

$$\ln K_M' = \ln [V_M'] + \ln [h^\circ] + \ln a_M \quad (12)$$

$$\ln K_{Al} = \ln a_{Al} + 3 \ln [h^\circ] + \ln [V_{Al}'''] \quad (13)$$

$$\ln K_a = 11 \ln a_{Al} + 17/2 \ln p_{O_2} + \ln a_M \quad (14)$$

Finally, there is the electroneutrality condition

$$[e'] + 2[O_i''] + [V_M'] + 3[V_{Al}'''] = [h^\circ] + 2[V_O^{\circ\circ}] + [M_i^\circ] \quad (15)$$

The equilibrium defect concentrations can now be calculated for each of the disorder types mentioned above. They are, of course, related to the values of two pertinent compositional parameters. One of these should obviously be the oxygen partial pressure, which can be controlled experimentally. The activity of the cation M can also be fixed at unity by proper selection of electrodes.

1) Disorder Dominated by  $M_i^\circ$  and  $O_i''$  (Anti-Schottky)

If the predominant defects are assumed to be  $e'$ ,  $h^\circ$ ,  $M_i^\circ$ , and  $O_i''$ , the required equations are (8), (9), (11), and (15). The latter may be simplified to

$$[e'] + 2[O_i''] = [h^\circ] + [M_i^\circ] \quad (16)$$

As this phase is known to be primarily an ionic conductor, it is reasonable to assume that this can be approximated at high values of  $p_{O_2}$  by

$$[M_i^\circ] = 2[O_i''] \quad (17)$$

However, as will be shown later, the dependence of the electron concentration upon the oxygen partial pressure is in the opposite direction as that of the oxygen interstitials, which were assumed to dominate the negative side of the electroneutrality condition (equation (16)). This means that at sufficiently low values of oxygen partial pressure the electron concentration will take the place of the oxygen interstitial concentration, and equation (16) can be best approximated by

$$[e'] = [M_i^{\circ}] . \quad (18)$$

Below this critical value of oxygen partial pressure the various equilibrium relations will therefore be modified.

2) Disorder Dominated by  $V_M'$  and  $V_O^{\circ\circ}$  (Schottky)

If the predominant defect types are assumed to be  $e'$ ,  $h^{\circ}$ ,  $V_M'$ , and  $V_O^{\circ\circ}$ , the required equations are (8), (10), (12), and a simplified form of (15):

$$[e'] + [V_M'] = [h^{\circ}] + 2 [V_O^{\circ\circ}] \quad (19)$$

which, for an ionic conductor at low and intermediate oxygen pressures can be approximated by

$$[V_M'] = 2 [V_O^{\circ\circ}] . \quad (20)$$

For reasons similar to those mentioned above, at high oxygen pressures equation (19) can be approximated by

$$[V_M'] = [h^{\circ}] . \quad (21)$$

3) Disorder Dominated by  $M_i^{\circ}$  and  $V_{Al}'''$  (Frenkel)

If the predominant defect types are assumed to be  $e'$ ,  $h^{\circ}$ ,  $M_i^{\circ}$ , and  $V_{Al}'''$  the required equations are (8), (11), (13), (14), and a simplified form of (15):

$$[e'] + 3 [V_{Al}'''] = [h^{\circ}] + [M_i^{\circ}] , \quad (22)$$

which, for an ionic conductor, can be assumed to be approximately

$$3 [V_{Al}'''] = [M_i^{\circ}] , \quad (23)$$

at intermediate and high oxygen pressures. At low oxygen pressures, the electron concentration becomes significant, and the electroneutrality condition becomes

$$[e'] = [M_i^{\circ}] . \quad (24)$$

The results from the solution of these sets of equations are given in Table III-1, and Figure III-6, assuming that  $a_M$  is unity.

#### INFLUENCE OF SUPPRESSED ELECTRONIC DISORDER

Three sets of assumptions relating to the predominant defect species present in phase of the  $\beta$  alumina type have been discussed. In each case the supposition was made that the electron and hole concentrations served to satisfy the requirement for electroneutrality when the positive and negative charges resulting from the presence of the primary ionic species were not equal. Furthermore, the functional dependence of the electronic defect species concentrations upon the oxygen partial pressure leads to the participation of one of them in the approximate form of the electroneutrality conditions under appropriate values of that compositional variable. This also predicts that the material will become an electronic conductor when the oxygen partial pressure approaches such values.

An alternative, and probably more realistic, approach when considering the  $\beta$  alumina phases is to consider that charge compensation might be accomplished by the presence of other ionic defect species instead of electrons or holes. This is similar to the phenomenon called "self-compensation" that occurs in certain compound semiconductors. The general rule to be kept in mind is that the defects of any given charge sign will be most prevalent that contribute the smallest value of free energy to the overall structure.

Because of the nature of the structure of the bridging layers and the very ionic behavior of  $\beta$  alumina phases, it is quite reasonable to expect that the M vacancies could form more readily than electrons, for example. The results of such an hypothesis will be discussed in some detail and it will be seen that it leads to a defect model that seems to be in qualitative accord with presently available experimental facts.

In this more ionic model (case 4) the predominant defects will be assumed to be  $V_M'$ ,  $M_i^{\circ}$ ,  $O_i''$ , and  $h^{\circ}$ . Electrons are also assumed to be present, but at lower concentrations than  $V_M'$ . The pertinent equations are therefore (8), (9), (11), (12), and an appropriate approximation of (15) involving the species mentioned above. At high values of oxygen pressure we

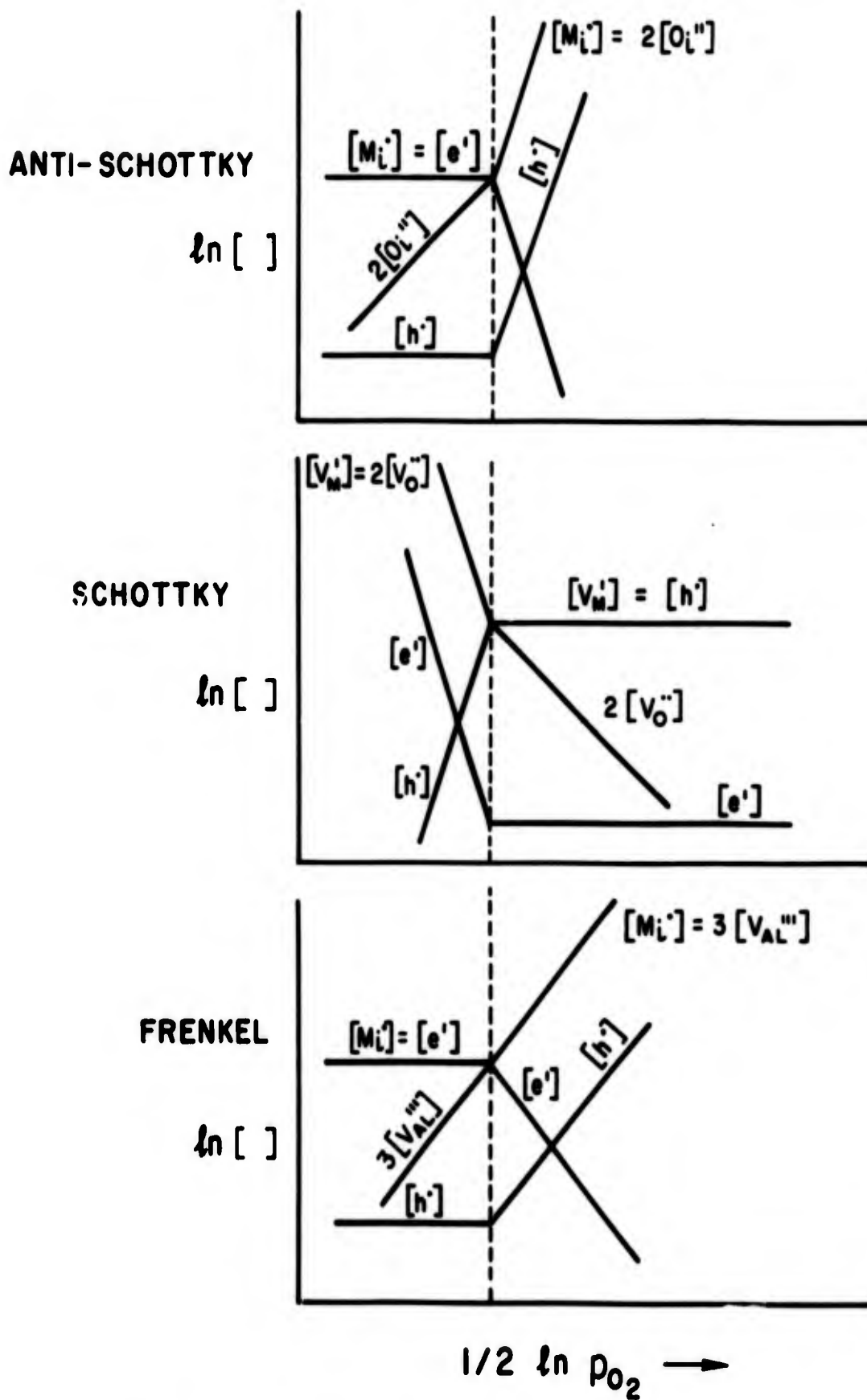


Figure III-6 Defect equilibrium diagrams for beta alumina

Table III-1 Defect Concentration as a Function of Oxygen Pressure

$$[A] \propto p_{O_2}^B$$

<u>A</u>	<u>B</u>	
<u>Type of Anti-Schottky Defect</u>	<u>Low <math>p_{O_2}</math></u>	<u>High <math>p_{O_2}</math></u>
$M_i^{\circ}$	0	1/6
$O_i''$	1/2	1/6
$h^{\circ}$	0	1/6
$e'$	0	- 1/6
<u>Type of Schottky Defect</u>		
$V_M'$	-1/6	0
$V_O^{\circ\circ}$	-1/6	-1/2
$h^{\circ}$	1/6	0
$e'$	-1/6	0
<u>Type of Frenkel Defect</u>		
$M_i^{\circ}$	0	17/44
$V_A'''$	17/44	17/44
$h^{\circ}$	0	17/44
$e'$	0	-17/44

can assume that (15) can be approximated by

$$[M_i^\circ] = 2 [O_i''] \quad (25)$$

as in Case I.

In that region of oxygen partial pressure simultaneous solution of these equations leads to the following expressions for the defect concentrations assuming that  $a_M$  is unity.

$$\ln [M_i^\circ] = 2/3 \ln K_M + 1/3 \ln K_O - 2/3 \ln K_e + 1/3 \ln 2 + 1/6 \ln p_{O_2} \quad (26)$$

$$\ln [O_i''] = 2/3 \ln K_M + 1/3 \ln K_O - 2/3 \ln K_e - 2/3 \ln 2 + 1/6 \ln p_{O_2} \quad (27)$$

$$\begin{aligned} \ln [V_M'] = 1/3 \ln K_M + \ln K_M' - 1/3 \ln K_O - 1/3 \ln K_e - 1/3 \ln 2 \\ - 1/6 \ln p_{O_2} \end{aligned} \quad (28)$$

$$\ln [h^\circ] = - 1/3 \ln K_M + 1/3 \ln K_O + 1/3 \ln K_e + 1/3 \ln 2 + 1/6 \ln p_{O_2} \quad (29)$$

$$\ln [e'] = 1/3 \ln K_M - 1/3 \ln K_O + 2/3 \ln K_e - 1/3 \ln 2 - 1/6 \ln p_{O_2} \quad (30)$$

It can be seen that as the oxygen partial pressure is reduced the M vacancy concentration increases, whereas the concentration of oxygen interstitials is reduced. At sufficiently low oxygen pressures the approximate electroneutrality expression becomes

$$[V_M'] = [M_i^\circ] \quad (31)$$

rather than that given by equation (18). Simultaneous solution with equations (8), (9), (11) and (12) then gives the following expressions for the defect concentrations in the low oxygen partial pressure regime.

$$\ln [M_i^\circ] = 1/2 \ln K_M + 1/2 \ln K_M' - 1/2 \ln K_e \quad (32)$$

$$\ln [O_i''] = \ln K_M - \ln K_M' + \ln K_O - \ln K_e + 1/2 \ln p_{O_2} \quad (33)$$

$$\ln [V_M'] = 1/2 \ln K_M + 1/2 \ln K_M' - 1/2 \ln K_e \quad (34)$$

$$\ln [h^\circ] = - 1/2 \ln K_M + 1/2 \ln K_M' + 1/2 \ln K_e \quad (35)$$

$$\ln [e'] = 1/2 \ln K_M - 1/2 \ln K_M' + 1/2 \ln K_e \quad (36)$$

These values are plotted schematically in the defect equilibrium diagram shown in Figure III-7.

The value of the oxygen partial pressure at the transition between the low oxygen pressure and high oxygen pressure regimes can be found by setting equations (26) and (28) equal to each other. The result is

$$\ln p_{O_2} \text{ (transition)} = - \ln K_M + 3 \ln K_M' - 2 \ln K_O + \ln K_e - 2 \ln 2 \quad (37)$$

Related modifications of the other two examples could be made in a similar manner. The result is that the M vacancy concentration can be assumed to merely replace the electron concentration, or on the other hand, oxygen vacancies replace holes. The details of those cases will not be included here however.

#### RELATION OF DEFECT EQUILIBRIA TO CONDUCTIVITY IN BETA ALUMINA PHASES

Various experimental observations concerning defect transport in various  $\beta$  aluminas are discussed elsewhere in this report, and there is no need to repeat them here. However, the correspondence between several hitherto puzzling aspects of those experiments and the predictions that result from consideration of the defect equilibria presented in this chapter should be mentioned.

The ionic conductivity has been found to be strongly dependent upon the oxygen partial pressure (increasing at higher values) with some cations, and not with others. In both cases, the ionic conductivity is much greater than the electronic conductivity. This may be rationalized by consideration of Figure III-7 if the transporting species are interstitial cations. The oxygen pressure dependence of the conductivity should depend upon the position of the experimental range of oxygen partial pressure with regard to the transition between the two regimes. Since the position of the transition will vary from one cation to another in accordance with equation (37), it is seen that such observations are not surprising.

Because of the temperature dependence of the constants in equation (37) it is also to be expected that the apparent activation energy for transport in

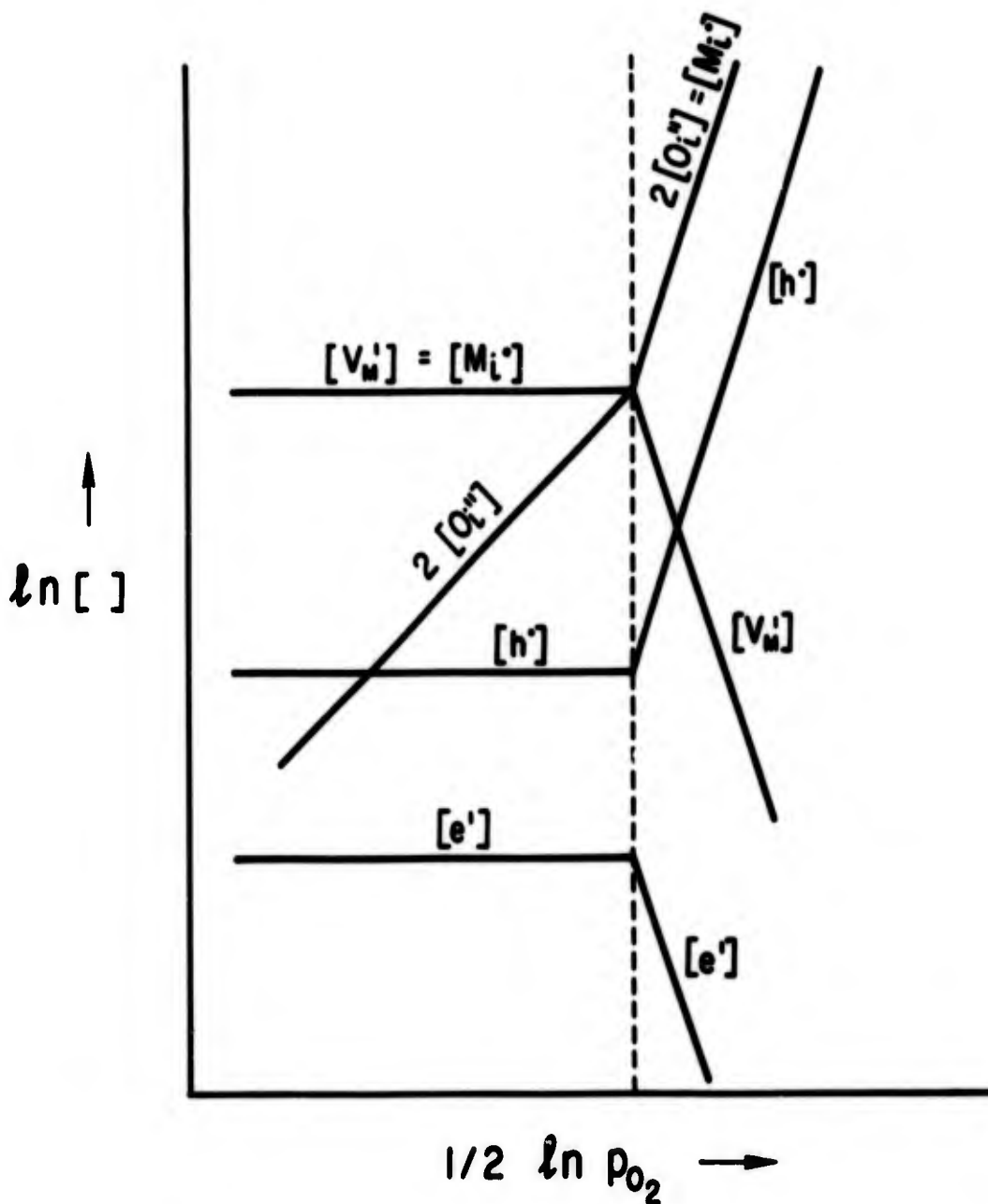


Figure III-7

Schematic defect equilibrium diagram for case in which M vacancy concentration is much greater than electron concentration.

samples which are in the oxygen-dependent regime will vary with temperature because of the interaction of both defect concentration and mobility considerations.

The independent experiment that showed that the hole conductivity is higher than the electron conductivity in copper  $\beta$  alumina is consistent with the higher hole concentration in Figure III-7.

Increasing ionic conductivity at higher oxygen partial pressure is also seen to be compatible with an M interstitial, but not an M vacancy mechanism.

## REFERENCES

1. H. Schmalzried and C. Wagner, Z. Phys. Chemie N.F. 31, 198 (1962).
2. H. Schmalzried, Prog. Solid State Chemistry 2, 265 (1965).
3. F. A. Kröger and H. J. Vink, Solid State Physics 3, 307 (1956).
4. F. A. Kröger, Chemistry of Imperfect Crystals, North-Holland Publishing Company (1964).
5. H. J. Vink, Festkörperprobleme IV, 205 (1965).
6. G. Brouwer, Philips Research Reports 9, 366 (1954).

CHAPTER IV

IONIC CONDUCTIVITY IN BETA ALUMINA PHASES  
CONTAINING SILVER AND THALLIUM

M.S. WHITTINGHAM

R.A. HUGGINS

## INTRODUCTION

As mentioned elsewhere in the Report, to determine the conductivity or any other structure-dependent property of a ternary system in a known and reproducible state, it is necessary to specify two compositional variables, such as the activities of two of the components. For  $\beta$  alumina  $\text{MA}_{11}^0\text{O}_{17}$ , an obvious choice is for one of these to be oxygen and the other the mobile species M. The activity of the former may be readily fixed at some known value simply by passing a gas of known composition over the specimen; the oxygen activity may be monitored by using a stabilized zirconia transducer. The activity of the latter is fixed at unity by having metal M in chemical equilibrium with the specimen.

To measure the ionic conductivity of the sample it is necessary to make two electrical contacts with it. Now, if one of these is reversible to the mobile species M, as required to fix the activity of M, then it is obviously possible to make both reversible so that the polarization problems associated with blocking electrodes are much reduced. The standard technique of using high frequency measurements to overcome contact polarization can be readily shown to be inapplicable with these materials, as their high ionic conductivity would require experimentally impossible high frequencies ( $>10^8$  Hz).

Two approaches were used to get reversible electrodes for samples containing either silver or thallium as component M. In the first, a molten nitrate of the metal M, in which some elemental M was immersed to fix the M activity, was placed in contact with the crystals. Electrical contact was then made with an electrode of M. In the second, either pure M itself or an alloy of M in solution in some low melting metal was used. The former has the advantage that the electrolyte is blocking to electrons and therefore only the conductivity associated with the  $\text{M}^+$  ion is measured. However, as will be discussed later, the use of molten salts was found unsatisfactory for a number of reasons. Thus the second alternative above had to be used.

To simplify this method it was desirable to use metals which are stable relative to their oxides at readily attainable oxygen partial pressures.

Silver and thallium were thus obvious choices. The oxygen partial pressure may easily be reduced sufficiently to prevent the formation of their oxides; this is not true for the alkali metals, that form  $\beta$  aluminas.

## EXPERIMENTAL METHODS

### Sample Preparation

Compressed pellets of  $\beta$  alumina were made by reacting  $\text{Na}_2\text{CO}_3$  and  $\text{Al}_2\text{O}_3$  together at an elevated temperature, as described elsewhere.

Polycrystalline pellets of silver  $\beta$  alumina were then prepared by cation exchange from sodium  $\beta$  alumina following the method of Yao and Kummer<sup>(1)</sup>. Arc emission spectroscopy showed very small quantities of residual sodium after this treatment. Ion exchange was accomplished in single crystal samples by the same method.

### Experimental Configurations

#### A) Liquid Electrodes for Polycrystalline Sample Experiments

Compressed pellets of  $\beta$  alumina were held in a quartz system as shown in Figure IV-1a. The outer liquid metal or salt level was kept below the top of the pellet to prevent any short circuiting between the two sections in the event of leakage. Contact with the liquid was made with wires. The oxygen activity over the two liquid surfaces was maintained at the same value.

#### B) Solid Metal Electrodes

For use with solid metal electrodes, single crystals were mounted in a quartz sample holder, as shown in Figure IV-1b. In the thallium case, thallium wire was simply placed between the crystal and a platinum sheet; this was sufficiently malleable even at room temperature to make good contact between the two surfaces. For silver, the two edges of the crystal were given a coating of silver metal using silver resinate solution and were then bonded to silver plates using the same solution. The other surfaces of the crystal were cleaned by nitric acid treatment. For measurements of the electronic component of the conductivity platinum electrodes, which are blocking to the mobile ions, were coated onto the sample edges using platinum resinate solution.

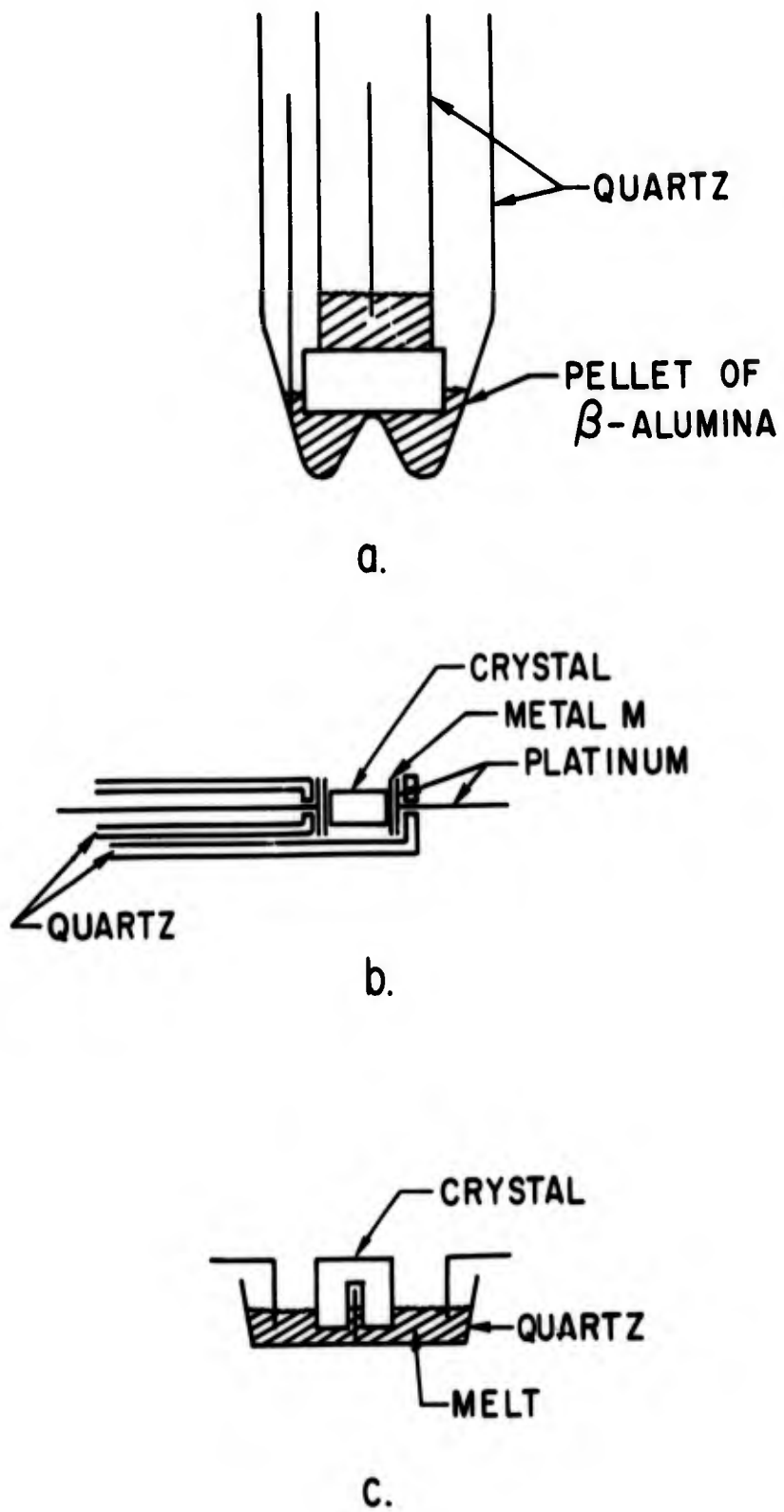


Figure IV-1 Experimental cell configurations

### C) Liquid Electrodes for Single Crystal Experiments

For use with liquid salts and liquid metal electrodes single crystals were cut into an inverted U-shape so as to dip into both compartments of the quartz cell depicted in Figure IV-1c. Metal or graphite leads were used as current contacts.

#### Conductivity Measurements

Both a.c. and d.c. equipment were used. Conventional instruments were used for d.c. measurements which allowed either the applied voltage or the current passed to be kept constant, while the other was monitored. For a.c. measurements a General Radio Company impedance bridge type 1608-A with a Hewlett Packard low frequency oscillator model 202CR was used.

### RESULTS

#### Molten Salt Experiments

All experiments with powder samples and molten salt electrodes failed because the pellets soaked up the molten salt and so short-circuited the cell. Even after sintering at 1750°C the density of the compressed pellets was only 85% of the x-ray density.

Experiments on single crystals in contact with molten salts were also unsuccessful because the surface of the crystal became coated with a thin film of the liquid salt before the conductivity could be measured over any significant temperature range. Because of this spreading of the contact the effective size of the crystal being measured also varied continuously. A third drawback was that the range of thermal stability of these salts is too small to derive an activation energy of the conduction process with any accuracy; frequently the melt would partially decompose during an experiment.

#### Liquid Metal Alloy Electrode Experiments

##### A) Polycrystalline Samples

Two different liquid metal solutions were used as electrodes. In one, silver was dissolved in molten gallium and in the other, copper was dissolved in molten tin. The purpose of these experiments was to see if

silver and/or copper could be electrically pumped into sodium  $\beta$  alumina to replace the sodium, so sodium  $\beta$  alumina pellets were used. Later x-ray analysis showed these samples to be a mixture of  $\beta$  and  $\beta'$  alumina.

In the silver experiments a black film was almost immediately formed on the surface of the melt and on the pellet. This was apparently not due to oxidation by the gaseous atmosphere, as the same occurred in pure hydrogen. In the absence of the  $\beta$  alumina no coloration of the melt was observed, so contamination was obviously due to interaction with the pellet. On a number of occasions it was also observed that a smoothly polished pellet 'grew' small solid bubbles on its surface, which were soluble in water to give an alkaline solution, merely on standing in air for a few days. These lumps were assumed to be  $\text{Na}_2\text{O}$ . No reproducible results were obtained with this system as in order to pass a steady current of 0.1 ma a continually increasing applied voltage was required.

Although the problems associated with degradation of the melt and pellet were less for the Cu/Sn experiment, the applied voltage again increased with time and never reached a constant value. In addition, the resistance of these samples was higher than might reasonably be expected for  $\beta$  alumina. The apparent initial resistance at 700°C was about 100,000 ohm-cm and this trebled over 15 hours.

#### B) Single Crystal Samples

Experiments on the two systems described above were repeated using single crystals of sodium and silver  $\beta$  alumina with the experimental configuration shown in Figure IV-1c. The results can be generalized as follows:

- 1) The resistance was higher than expected by two to three orders of magnitude.
- 2) The activation energy for the conduction process was unreproducible and greater than 20 kcal/mole.
- 3) The resistance was sometimes frequency dependent and only when very high was it independent of the frequency.
- 4) There was no obvious difference between measurements on the two  $\beta$  aluminas.

- 5) The samples used with the Ag/Ga melt frequently showed metallic luster inside the crystal which could not be removed by chemical means.
- 6) The results were quantitatively unreproducible from day to day on a given sample.
- 7) X-ray fluorescence analysis of the sample which showed the metallic luster described above indicated the presence of 10% by wt of both Ga and Ag.

#### Pure Metal Electrode Experiments

##### A) Silver $\beta$ Alumina

Single crystals of silver  $\beta$  alumina were measured using the experimental set up shown in Figure IV-1b. A typical set of results is shown in Figure IV-2; the numbers on the lines indicates the measurement sequence. The general characteristics of these results can be summarized as:

- 1) The resistance was frequency independent from d.c. to 10,000 Hz provided the current density was kept fairly low, less than about  $5 \text{ mA/cm}^2$ .
- 2) The results were reproducible for lines such as 1 and 2 only if the temperature was kept below about  $400^\circ\text{C}$ . Above that temperature the samples were obviously changing with time. Equilibration at higher temperatures produced the results indicated by line 3. They were then reproducible over the entire temperature range from day to day on any given sample. The temperature of the sudden discontinuity in both slope and magnitude observed in the early runs always occurred at about  $175^\circ\text{C}$ .
- 3) There were indications that if the crystal was held at an elevated temperature for a prolonged period silver metal precipitated upon cleavage planes of the crystal. This was indicated by both visual presence of silver and by the presence of 'Newton's Rings'.
- 4) At elevated temperatures silver also tended to precipitate along the edges of the crystal, thus short-circuiting the cell.

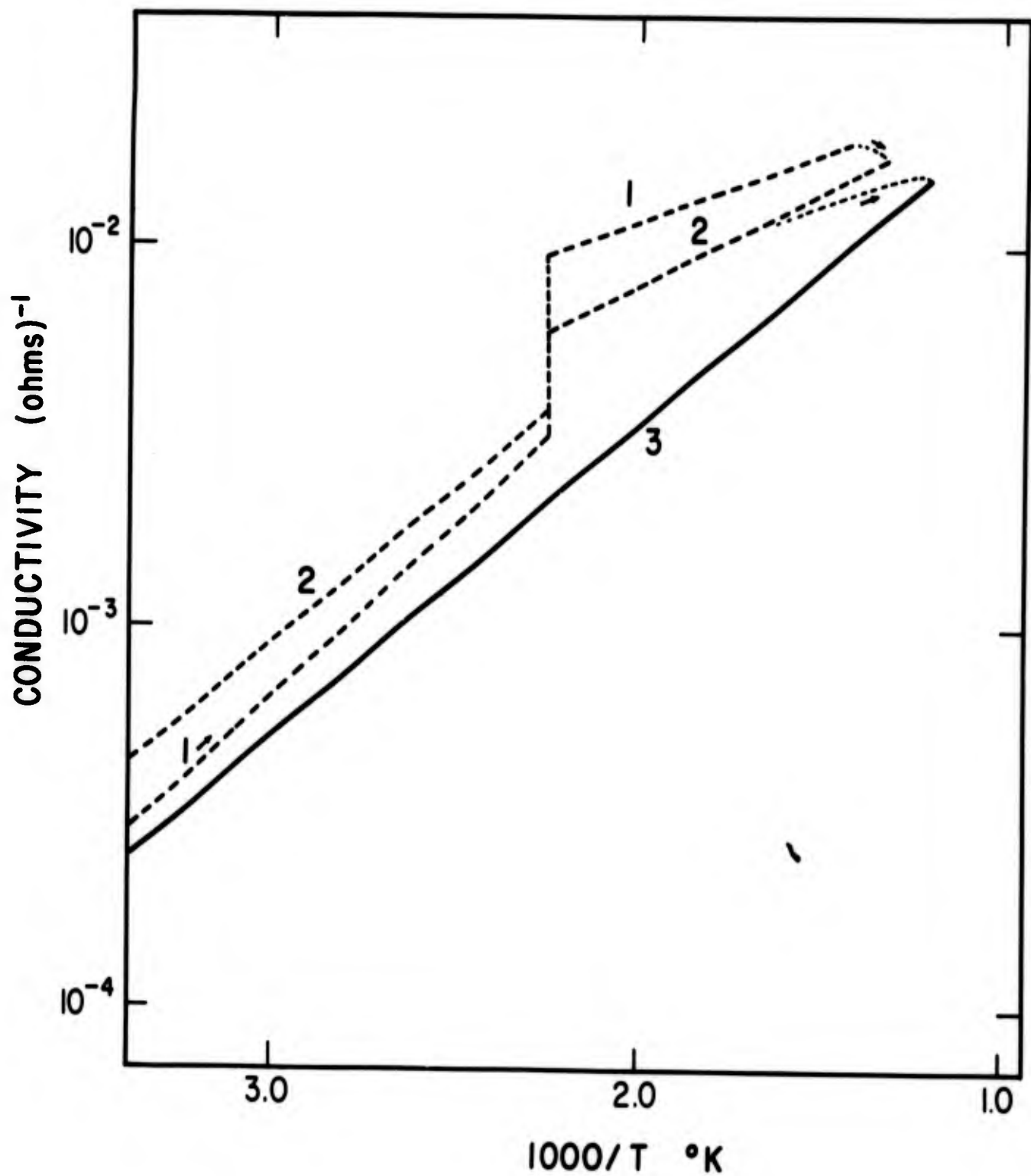


Figure IV-2 Conductivity results for silver beta alumina

- 5) If the crystal was heated above about 900°C in the preparation of its surfaces it decomposed to give a white opaque material which flaked rather readily.
- 6) The final value of the temperature dependence always fell between the slopes of the upper and lower portions of the initial experimental data (line 1).
- 7) The absolute value of the conductivity varied by half an order of magnitude from sample to sample at room temperature.
- 8) The variation of conductivity with the ambient oxygen partial pressure was evaluated at 600°C. The conductivity increased by about 5% when the oxygen partial pressure was increased from less than  $10^{-20}$  atmospheres to that of air. This is believed to be within the experimental error of the measurement, however.

#### B) Thallium $\beta$ Alumina

Conductivity measurements of single crystals of thallium  $\beta$  alumina were frequency independent provided the oxygen partial pressure was kept low enough to prevent the formation of oxides of thallium. They were very dependent upon frequency if any oxide was present.

Single crystals of thallium  $\beta$  alumina mounted in the sample holder of type 1b with solid electrodes gave reasonably reproducible results. However, samples were invariably covered with a thin film of black material, presumably thallium oxide, when removed from the sample holder. Both the apparent activation energy and the conductivity were higher than expected, however, and it is suspected that this surface layer may have been participating in the conduction process.

Other experiments were carried out using the cell in Figure IV-1c with molten thallium electrodes and graphite current contacts. The results obtained were fairly reproducible over the short term (a few days) but over longer periods thallium tended to spread over the sample.

The conductivity results, together with those for the silver sample are given in Figure IV-3. The electronic component of the conductivity of samples of sodium and silver  $\beta$  alumina, measured by using platinum electrodes which are blocking to the ions, are also shown in that figure.

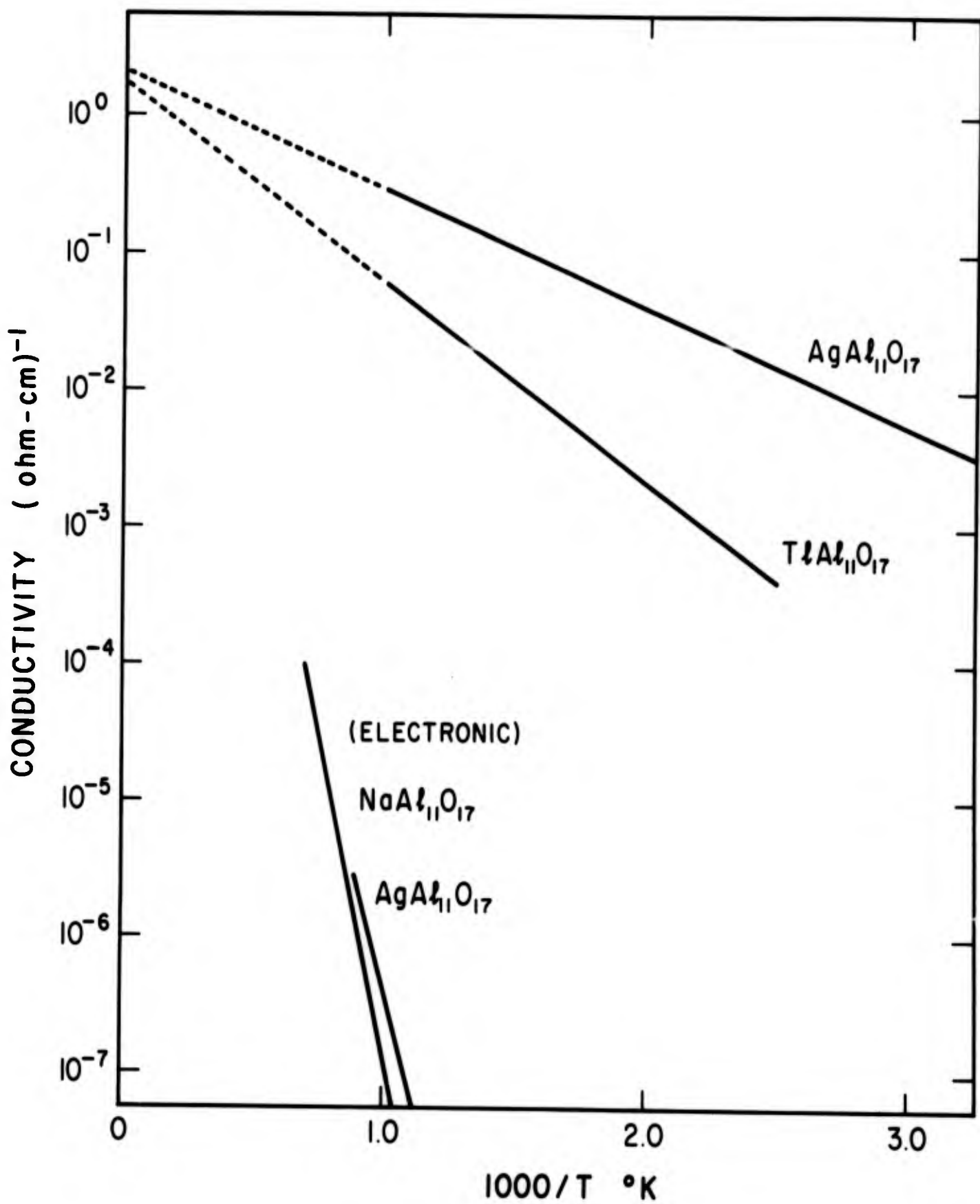


Figure IV-3 Conductivity results for beta alumina

## DISCUSSION

The results of the measurements using liquid metal solutions as electrodes indicate that satisfactory results cannot be obtained at present using this technique for reasons not altogether understood. The blocking of the ions may be due to a number of reasons, such as non-wetting of the crystal surface or the formation of an oxide layer at the interface. Recent work<sup>(2)</sup> has shown that Ga (I) is readily soluble in  $\beta$  alumina as well as indicating that gallium may cause the decomposition of this phase to form a phase with the corundum structure.

The results obtained using pure metal electrodes were much better. The electrodes were reversible, the resistance and activation energies were low and the results were reproducible on any given sample. The non-equilibrium behavior observed upon initial measurements of silver  $\beta$  alumina illustrated by Figure IV-2 and the significance of the sudden change in both slope and magnitude at about 175°C are not known but may be associated with surface silver species and the thermal stability of the Ag-O bond.

The values of the observed activation energies for ionic conductivity in silver and thallium  $\beta$  alumina, determined from plots of  $\log \sigma T$  versus  $1/T$ , 4.6 and 7.6 kcal/mole respectively, are in reasonably good agreement with those determined by radioactive tracer methods<sup>(1)</sup>. The latter values are 4.05 kcal/mole for silver, and 7.18 kcal/mole for rubidium, which has an ionic radius only slightly greater than thallium.

The measured values of ionic conductivity are lower than expected from the reported<sup>(1)</sup> value for sodium  $\beta$  alumina at room temperatures,  $3 \times 10^{-2} \text{ (ohm-cm)}^{-1}$ . Figure IV-3 shows that the conductivities approach each other as  $1/T \rightarrow 0$  as generally expected for compounds with the same crystal structure and number and charge of carriers. Although the experimental arrangement was such that the electronic component of the total charge flux would also be measured, the results obtained for the separate electronic conductivity of both silver and sodium  $\beta$  alumina indicate that the electronic contribution to the total conductivity is very small, less than one part in  $10^6$  below 500°C.

The observation that the conductivity of the silver sample is essentially independent of the oxygen partial pressure is in accordance with the discussion of defects in such structures presented in Chapter III.

REFERENCES

1. Y. Y. Yao and J. T. Kummer, J. Inorg. Nucl. Chem. 29,  
2453 (1967).
2. R. H. Radzilowski, Inorg. Chem. 8, 994 (1969).

CHAPTER V

IONIC TRANSPORT IN BETA ALUMINA PHASES  
CONTAINING SODIUM AND COPPER

R.W. HELLIWELL

R.A. HUGGINS

## INTRODUCTION

This chapter is a preliminary report on a group of measurements and observations relating to ionic transport in  $\beta$  alumina phases containing either sodium or copper as the cation, M.

In both of these cases the situation is considerably more complicated than in those discussed in Chapter IV. The electrode problem was found to be particularly troublesome in the case of samples containing sodium. Those containing copper have shown a very strong dependence of the apparent conductivity upon the ambient oxygen activity.

The studies were done with both single crystals and polycrystalline specimens.

## POLYCRYSTALLINE SAMPLE PREPARATION

Synthesis of polycrystalline sodium  $\beta$  alumina was performed by mixing finely divided powders of  $\text{NaAlO}_2$  and  $\text{Al}_2\text{O}_3$ , pressing into pellets, and sintering at about  $1550^\circ\text{C}$  for one hour. The sintered pellets had a resultant density of 75% to 85% of theoretical density with the samples which had the greatest sodium concentration being the most dense. Samples were mixed with a variety of Na/Al ratios from 0.08 to 0.30.

Those samples which contained only the  $\beta$  alumina phases were used in subsequent tests. X-ray analysis was used to detect the presence of additional phases such as  $\text{Al}_2\text{O}_3$  or  $\text{NaAlO}_2$  as well as to identify the  $\beta$  alumina phases present. In all samples produced by the above method, there was evidence for both the sodium  $\beta$  and  $\beta''$  phases.

The synthesis of polycrystalline copper  $\beta$  alumina was attempted by similar methods in the temperature range from  $1200^\circ\text{C}$  to  $2000^\circ\text{C}$ . All efforts using  $\text{Al}_2\text{O}_3$  and either  $\text{Cu}_2\text{O}$  or  $\text{CuAlO}_2$  as starting materials have failed. Copper  $\beta$  alumina which was subsequently produced by ion exchange of sodium  $\beta$  alumina, when brought to  $1750^\circ\text{C}$ , spontaneously decomposed into  $\text{Al}_2\text{O}_3$  and  $\text{Cu}_2\text{O}$ , a fact which makes clear the reason for failures in synthesizing copper  $\beta$  alumina.

Sodium  $\beta$  alumina pellets were converted to copper  $\beta$  alumina using the

ion exchange method described by Yao and Kummer<sup>(1)</sup>. This process involves immersing pellets of polycrystalline sodium  $\beta$  alumina in molten  $\text{CuCl}$  at  $500^\circ\text{C}$  to  $550^\circ\text{C}$  in a relatively oxygen free atmosphere. Early experiments were carried out in commercially prepared reagent grade  $\text{CuCl}$  procured from several chemical supply companies. These experiments resulted in no significant ion exchange. It was found that the activity of copper in the liquid  $\text{CuCl}$  was low, and that a substantial amount of copper metal would dissolve in the liquid. Oxide impurities were also found to be present.

Subsequent ion exchange experiments were performed in  $\text{CuCl}$  which had been purified by sublimation after being saturated with copper. A piece of copper metal was placed in the  $\text{CuCl}$  ion exchange both to insure that the copper activity remained fixed at unity. The result was that the exchange of copper ions for sodium ions was achieved in  $\beta$  alumina. X-ray fluorescence analysis was used on the copper  $\beta$  alumina specimens, but did not establish the copper concentration with sufficient precision to specify the amount of retained sodium, if any.

The polycrystalline copper  $\beta$  alumina samples were brown, compared with white for sodium  $\beta$  alumina. Chemical tests indicated that the brown color was due to the presence of a second copper-containing phase. The brown color was uniform in density throughout samples which had been thoroughly exchanged.

#### ELECTRICAL TRANSPORT MEASUREMENTS UPON POLYCRYSTALLINE SODIUM BETA ALUMINA

Electrical transport measurements were performed on the samples of sintered polycrystalline sodium  $\beta$  aluminas described previously throughout a range of temperatures. The samples were coated with platinum on the two opposite parallel faces by applying platinum resinate (Engelhard # A 1121) and heating to  $300^\circ\text{C}$  to form a platinum film. Successive coatings were administered until the resulting platinum layer was electrically continuous. These films adhered well to all samples.

Conductances were measured using both a c and d c techniques. Most measurements were performed with a General Radio 1608 A impedance bridge. The conductivity of polycrystalline specimens was found to depend upon the

initial composition, as shown in Figure V-1. These measurements were made at 10 kHz at an applied rms potential difference of about 0.1 volts. As mentioned above, it is probable that both  $\beta$  and  $\beta''$  phases were present in these specimens, and on the composition extremes other phases may also be present, so no direct explanation of the conductivity variances with composition can be made.

It should be emphasized that the platinum electrodes are blocking to ions, so alternating current measurements over a range of frequencies were performed to determine whether polarization effects could be eliminated. Even the highest frequency used (20 kHz) was not sufficiently high to render electrode polarization effects negligible, as indicated by the fact that the results were still frequency dependent. The measured values of the conductivity should, therefore, be regarded as lower than the real values.

The temperature dependence of the apparent conductivity of the sodium  $\beta$  aluminas is given in Figure V-2. The values of conductivity shown in Figures V-1 and V-2 are for initial measurements. Subsequent measurements on the same samples varied somewhat, generally drifting toward lower values. Equilibration with a different atmosphere, or the same atmosphere at different temperatures, is expected to produce different defect concentrations, and, therefore, different values of the conductivity as discussed in Chapter III. Equilibration or re-equilibration of specimens during the measurement process may have taken place.

The apparent activation energy for conduction in sodium  $\beta$  alumina, determined from plots of  $\log \sigma T$  versus  $1/T$ , was found to be approximately 9700 cal/mole in the range from 150°C to 250°C, gradually decreasing with increasing temperatures to approximately 5800 cal/mole in the range from 500°C to 650°C, the highest temperature range over which measurements were made.

An attempt was made to provide liquid sodium metal electrodes which would be reversible to both ions and electrons. The apparent conductivity values obtained were slightly lower with sodium electrodes than with platinum electrodes, probably due to the formation of  $\text{Na}_2\text{O}$  at the interface. Furthermore, experimental problems involving containment of the liquid sodium were

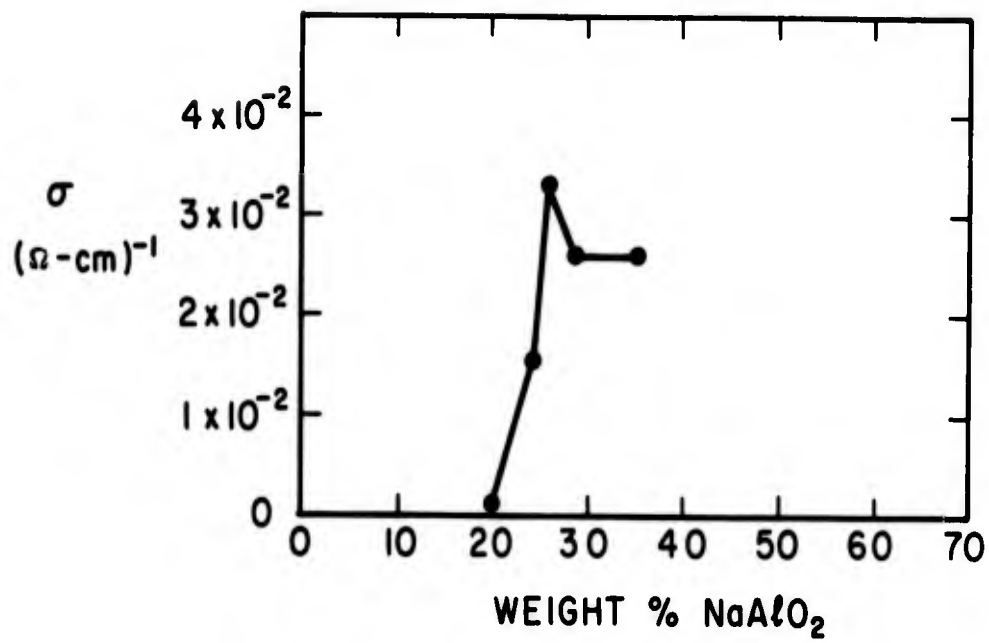


Figure V-1 Conductivity vs initial composition of sodium beta alumina at 352°C (10 KHz, 0.1 rms volts, platinum electrodes).

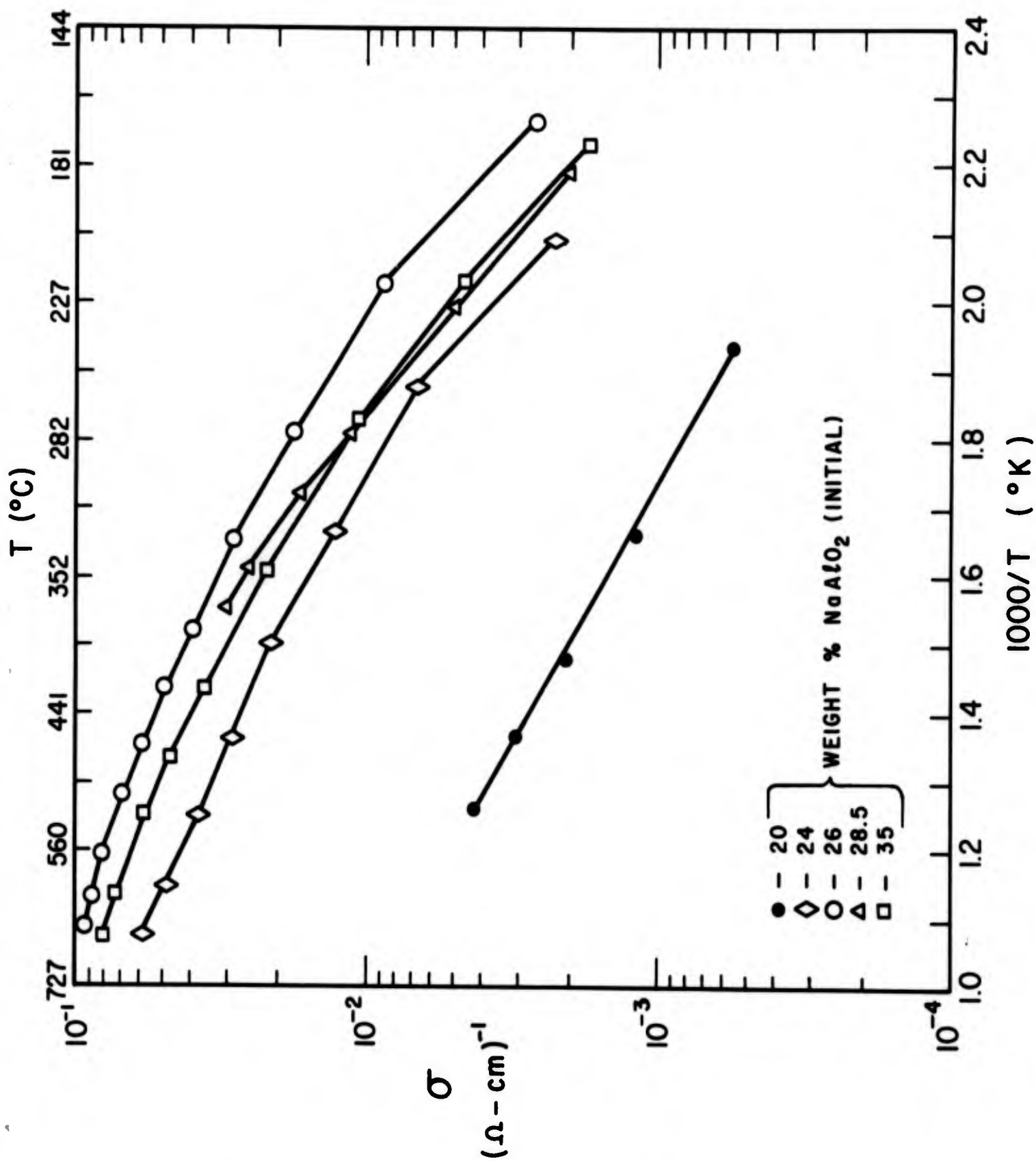


Figure V-2 Conductivity of sodium beta alumina.  
(10 kHz, 0.1 rms volts, platinum electrodes).

so great that further experiments along this line were not attempted.

In order to evaluate the electronic contribution to the total measured conductivity, direct current measurements were made on sodium  $\beta$  alumina specimens using platinum electrodes, which are blocking to ions if the decomposition potential is not exceeded. The electronic conductivity measured by this means was very low compared to the total conductivity, being less than 0.1% of the total at all temperatures for which the measurements were made.

#### ELECTRICAL TRANSPORT MEASUREMENTS UPON COPPER BETA ALUMINA

It was found that the conductivity of samples of sintered polycrystalline copper  $\beta$  alumina, prepared as described earlier, was strongly dependent upon the oxygen activity.

To investigate this effect, samples were allowed to come to equilibrium with various values of oxygen activity in the environment at elevated temperatures. They were then cooled rapidly to considerably lower temperatures where they were assumed to be stable, but no longer in equilibrium. Conductance measurements were then made as a function of temperature (with the maximum temperature limited to values below which re-equilibration appeared to proceed rapidly). This group of experiments was carried out by making alternating current measurements on samples of copper  $\beta$  alumina with platinum electrodes.

Isothermal equilibration kinetics were measured at 850°C. A sample was first equilibrated with a purified helium atmosphere containing an oxygen activity of less than  $10^{-20}$ . (The activity was measured by use of a zirconia transducer in sample envelopes similar to the one used in this experiment.) The atmosphere was then changed to air, and the conductivity was measured as a function of time. The conductivity was found to increase with time from its initial value toward a higher plateau, as shown in Figure V-3. After 800 minutes, the conductivity was essentially stabilized at about 17 times the original value. Re-equilibration with the lower oxygen activity was also studied, and approximately the same kinetic results obtained. Experiments in both directions were performed several times on the same sample

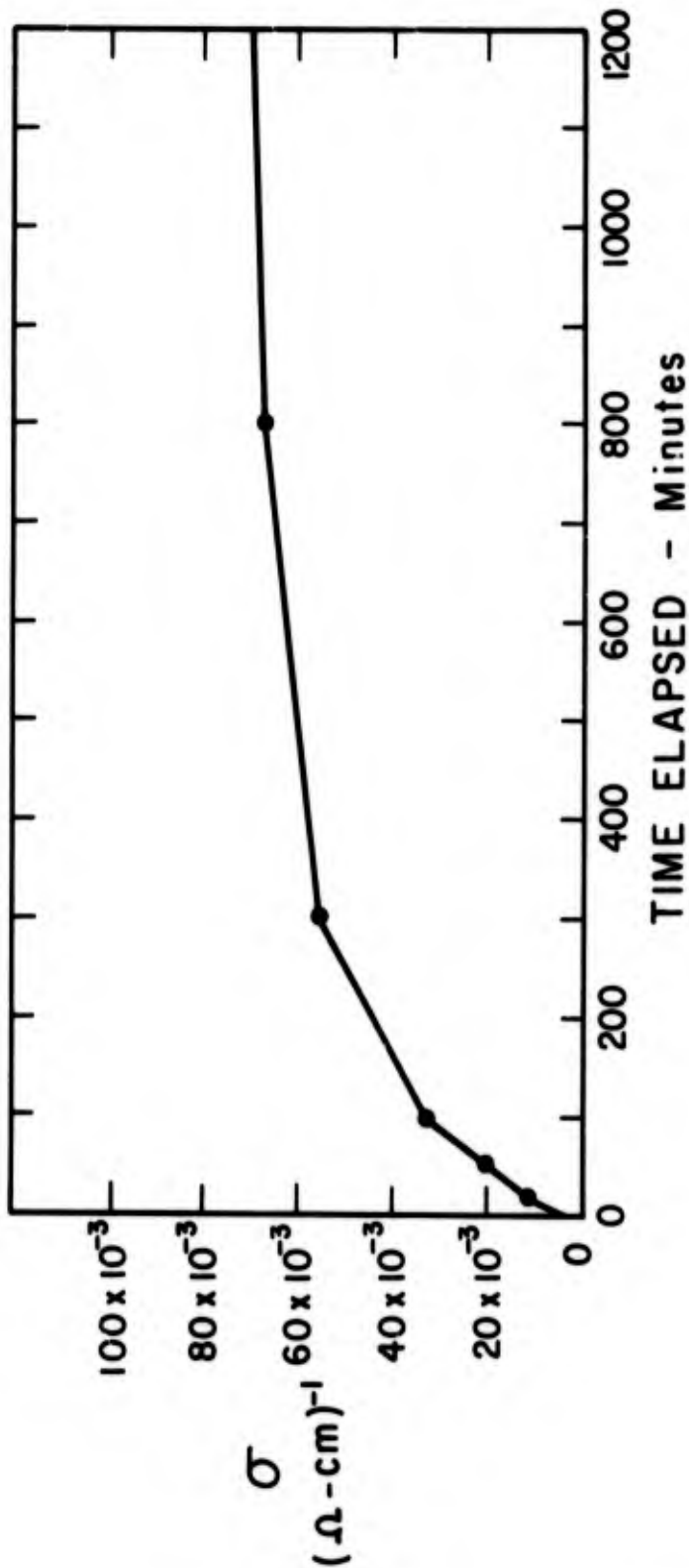
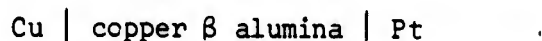


Figure V-3 Conductivity of copper beta alumina vs time elapsed after air was admitted to sample chamber, with sample initially equilibrated in purified helium ( $p_{O_2} \approx 10^{-20}$  atmos.) (10 kHz, 0.1 rms volts, platinum electrodes).

and were found to be reproducible.

The effect of the oxygen activity with which a sample was equilibrated at a high temperature (845°C) upon the conductivity at significantly lower temperatures is illustrated in Figure V-4. The activation energies for conduction were determined from  $\log \sigma T$  versus  $1/T$  plots. The air equilibration resulted in an activation energy of approximately 5000 cal/mole, and the low oxygen activity equilibration resulted in an activation energy of approximately 25,900 cal/mole.

The partial conductivities of the two electronic species, electrons and holes, were determined on a polycrystalline sample of copper  $\beta$  alumina according to the method first proposed by Wagner<sup>(2)</sup> using the cell

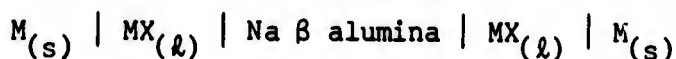


at 850°C. The data were analyzed and plotted in the manner suggested by Patterson, Bogren and Rapp<sup>(3)</sup>. The results are shown in Figure V-5. The slope of the resulting curve gives the value of the hole partial conductivity which was found to be  $4.8 \times 10^{-3} (\text{Ohm} \cdot \text{cm})^{-1}$  at that temperature. The electronic partial conductivity, found from the intercept with the vertical axis, was  $1.5 \times 10^{-8} (\text{Ohm} \cdot \text{cm})^{-1}$ .

#### PRODUCTION OF COPPER BETA ALUMINA BY ELECTRICALLY DRIVEN TRANSPORT

The mobile sodium ions in sodium  $\beta$  alumina crystals can be exchanged with numerous monovalent and divalent cations by immersion in a molten salt, as reported by Yao and Kummer<sup>(1)</sup>. As mentioned earlier in this chapter, copper can also be exchanged, at least partially, with sodium in the  $\beta$  alumina structure by this method.

A different and more general method was developed using electrically driven ion transport to force the exchange reaction to proceed in the desired direction. Single crystals of copper  $\beta$  alumina have been produced by this method. Sodium  $\beta$  alumina single crystals were provided with electrodes reversible to the ions to be transferred, through which mobile ions entered and left the crystal. The cell



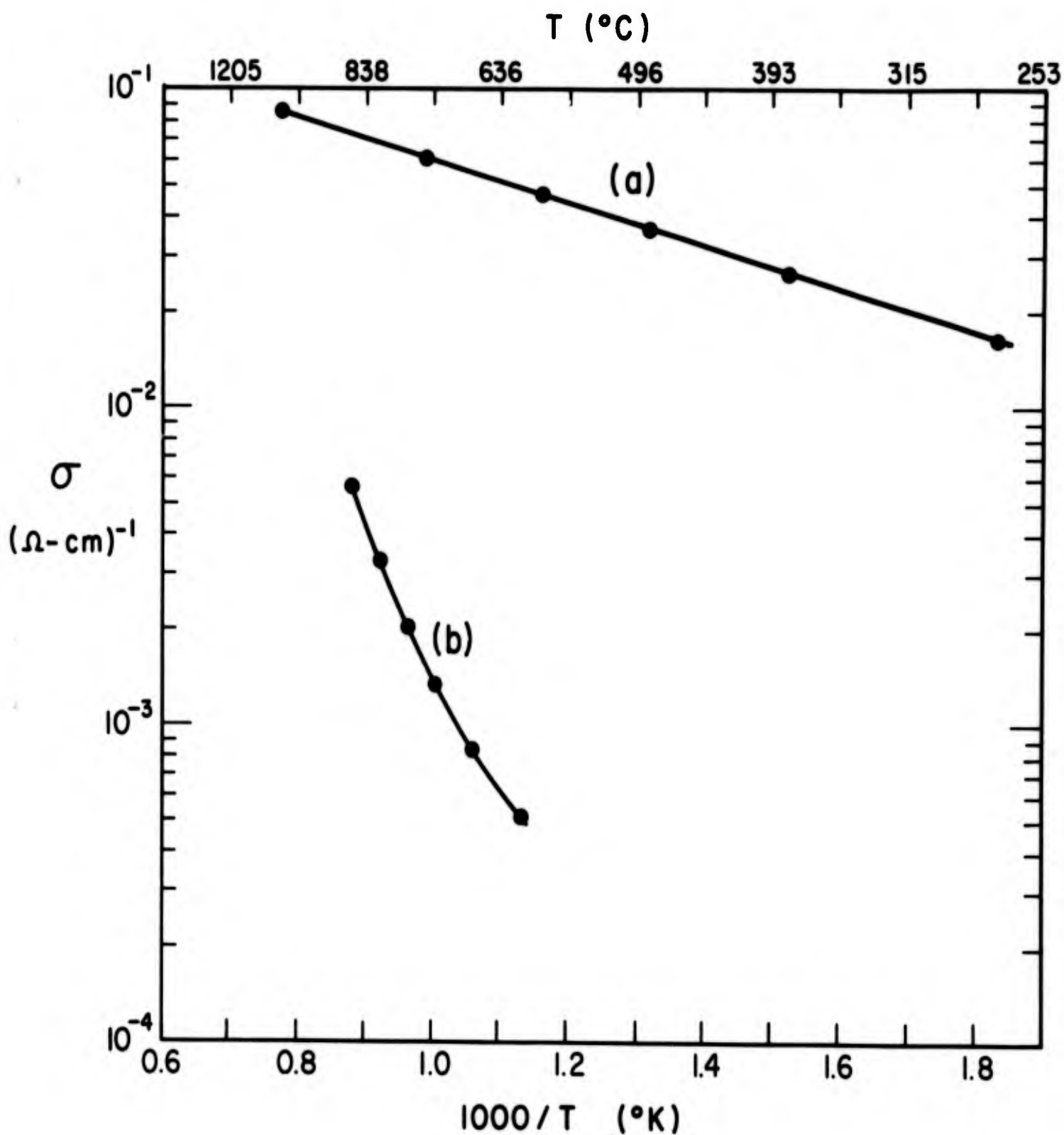


Figure V-4 Conductivity of copper beta alumina  
 (10 kHz, 0.1 rms volts, platinum electrodes).  
 a) Equilibrated in air ( $p_{O_2} \approx 0.2$  atmos.)  
 b) Equilibrated in purified helium ( $p_{O_2} \approx 10^{-20}$  atmos.)  
 Both quenched prior to conductivity measurements.

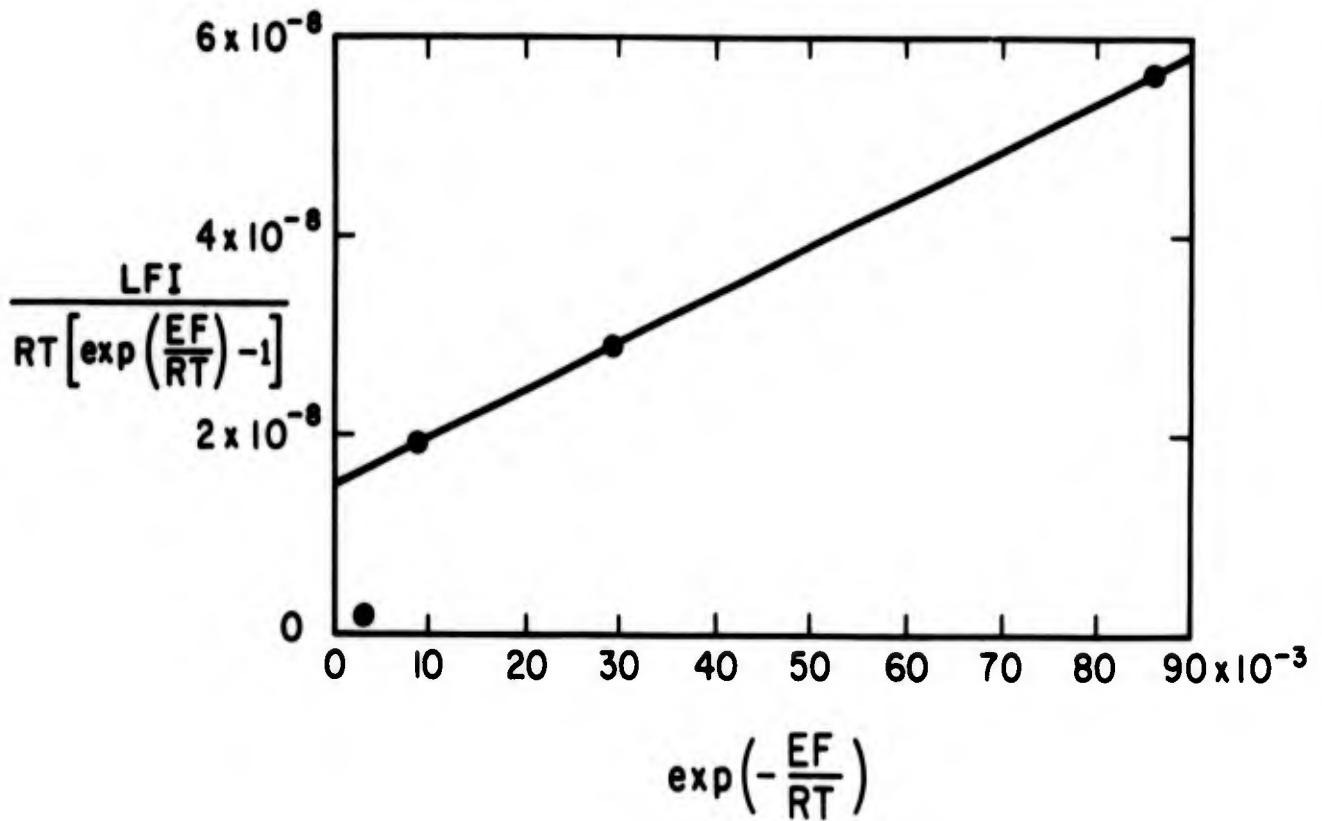


Figure V-5 Potential difference vs steady state current, plotted in the manner suggested by Patterson, Bogren and Rapp<sup>(3)</sup>.

was subjected to a potential difference.  $M^+$  ions enter the  $\beta$  alumina at the positive electrode and  $Na^+$  ions initially present leave at the negative electrode. The subscripts on the cell symbols denote solid and liquid phases. Both copper and silver  $\beta$  alumina crystals have been produced by this method, using liquid  $CuBr$  and  $AgNO_3$  respectively.

Liquid salt electrodes were selected because a satisfactory sample-electrode interface is easily formed, and the liquid salts act as reservoirs for the displaced  $Na^+$  ions. An experimental configuration using liquid salt electrodes and a U shaped crystal is shown in Figure V-6.

The copper  $\beta$  alumina produced with a one volt potential difference in a purified helium atmosphere was dark green in color, with evidence of metallic copper precipitate at visible imperfections. During the exchange process, the portion containing the copper ions was clearly distinguished from that containing mostly sodium, which is colorless, by a relatively sharp visible boundary. This color boundary passes through the crystal during the exchange process, moving from the positive electrode toward the negative electrode. The direction of the boundary movement can be explained only by  $M^+$  ions entering the crystal at the positive electrode, rather than by anions entering the crystal at the negative electrode.

The amount of total charge transfer necessary to completely exchange the  $Na$  with  $Cu$  may be compared with experiment by using the equation:

$$q = n z F$$

where

$$\begin{aligned} q &= \text{amount of charge passed in cell} \\ n &= \text{number of moles of } M^+ \text{ in specimens} \\ z &= \text{valence of cation} = 1 \\ F &= \text{Faraday constant} \end{aligned}$$

It was found that the exchange was essentially complete after the calculated amount of charge had passed through the cell.

When a single crystal was transformed from sodium to copper  $\beta$  alumina in this manner, the lattice parameter  $C_0$  was found to decrease from 22.523 Å to 22.447 Å. The ionic conductivity was also found to decrease by a factor of 0.3 at 540°C.

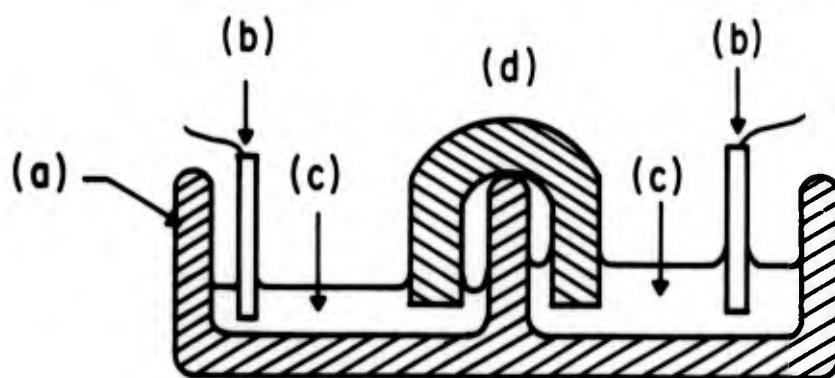


Figure V-6 Cutaway diagram of cell used to exchange ions in  $\beta$  alumina by means of an electrical driving force. The labelled parts of the cell are:

- a) Double chambered fused silica reservoir.
- b) Metal M electrodes.
- c) Molten salt MX.
- d) Beta alumina crystal cut to inverted U.

The resulting copper precipitate may be explained by the fact that the phase field of copper  $\beta$  alumina is narrower than that of sodium  $\beta$  alumina at any given temperature, as predicted in Chapter III. Thus, a copper rich phase must be rejected.

The green color is probably due to the presence of a colloidal copper precipitate. Magnetic susceptibility measurements did not detect the paramagnetic cupric ion. Green samples of copper  $\beta$  alumina were found to be diamagnetic, with about the same susceptibility as sodium  $\beta$  alumina,  $\psi_m = - 0.354 \times 10^{-6}$  e m u/gm.

#### REFERENCES

1. Y. Y. Yao and J. T. Kummer, J. Inorg. Nucl. Chem. 29, 2453 (1967).
2. C. Wagner, Proc. Int. Comm. Electrochem. Thermo. and Kinetics CITCE, 7th Meeting, London, 1955, Butterworth Scientific Publications, London, (1957).
3. J. W. Patterson, E. C. Bogren, and R. A. Rapp, J. Electrochem. Soc.: Solid State Science, 752 (1967).

Unclassified

Security Classification

DOCUMENT CONTROL DATA - R & D

(Security classification of title, body of abstract and indexing annotation must be entered when the overall report is classified)

1. ORIGINATING ACTIVITY (Corporate author)		2a. REPORT SECURITY CLASSIFICATION	
Department of Materials Science Stanford University Stanford, California 94305		Unclassified	
3. REPORT TITLE		2b. GROUP	
USE OF SOLID STATE ELECTROCHEMICAL TRANSDUCER TECHNIQUES FOR CONTROL OF THE POINT DEFECT STRUCTURE IN SOLIDS			
4. DESCRIPTIVE NOTES (Type of report and inclusive dates)			
Final technical report			
5. AUTHOR(S) (First name, middle initial, last name)			
M.S. Whittingham, R.W. Helliwell, and R.A. Huggins			
6. REPORT DATE	7a. TOTAL NO. OF PAGES	7b. NO. OF REFS	
June, 1969			
8a. CONTRACT OR GRANT NO.	9a. ORIGINATOR'S REPORT NUMBER(S)		
N00014-67-0112-0020	SU-DMS-69-R-64		
b. PROJECT NO.	9b. OTHER REPORT NO(S) (Any other numbers that may be assigned this report)		
NR 032-506			
c.			
d.			
10. DISTRIBUTION STATEMENT			
Reproduction in whole or in part is permitted for any purpose of the United States Government. Distribution of this document is unlimited.			
11. SUPPLEMENTARY NOTES		12. SPONSORING MILITARY ACTIVITY	
		Office of Naval Research	
13. ABSTRACT			
<p>Studies of the crystal structure and ionic transport in materials containing beta alumina and related phases are reported. Beta alumina has the nominal formula <math>M Al_{11} O_{17}</math>, where M is Li, Na, K, <math>NH_4</math>, Ag, or Tl. The structure of the adjacent <math>M_2O</math>-rich phase was studied and found to have an analogous structure consisting of dense blocks with the gamma alumina structure separated by low-density bridging layers containing M ions. Unusually rapid ionic transport along these bridging layers was found, and defect models appropriate to such systems discussed.</p>			

Unclassified

Security Classification

14 KEY WORDS	LINK A		LINK B		LINK C	
	ROLE	WT	ROLE	WT	ROLE	WT
defects						
electrochemistry						
ionic conductivity						
x-ray						
beta alumina						
ionic defect equilibria						